

Design Methodologies for the Seismic Retrofitting of Bridges

by

Alexander A Otenti

B.S. Civil and Environmental Engineering 2003  
Worcester Polytechnic Institute

Submitted to the Department of Civil and Environmental Engineering  
in Partial Fulfillment of the Requirements for the Degree  
of Master of Engineering in Civil and Environmental Engineering

at the

Massachusetts Institute of Technology

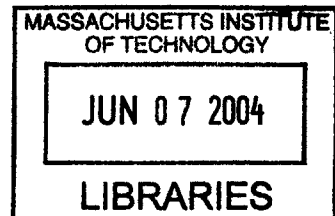
June 2004

©2004 Massachusetts Institute of Technology  
All rights reserved

Signature of Author.....  
Department of Civil and Environmental Engineering  
May 7, 2004

Certified by.....  
Dr. Jerome J Connor  
Professor of Civil and Environmental Engineering  
Thesis Supervisor

Accepted by.....  
Heidi Nepf  
Chairman, Committee for Graduate Students



BARKER



# Design Methodologies for the Seismic Retrofitting of Bridges

by

Alexander A Otenti

B.S. Civil and Environmental Engineering 2003  
Worcester Polytechnic Institute

Submitted to the Department of Civil and Environmental Engineering  
on May 7, 2004 in Partial Fulfillment of the Requirements for the Degree  
of Master of Engineering in Civil and Environmental Engineering

## Abstract:

This paper formulates an earthquake design strategy for bridges. Earthquakes can cause extreme economic damage and loss of life. Structural engineers must be conscience of earthquake slip type, earthquake proximity, and local soil properties when designing a structure. Structures subjected to near-field seismic events feel much complex motions and frequencies than those subjected to far-field events. When designing a structure in a seismic zone it is crucial that the engineer examine a sample of previous earthquake records from the region. Earthquake data is organized into response spectra, time histories, and frequency histories. Response spectra display the spectral displacement, velocity, and acceleration in terms of periods and are of the most interest to structural engineers. Once all of the data is gathered and organized it is necessary to decide on a retrofit strategy. Retrofitting involves either strengthening the bridge or shifting the period out of the power range of the earthquake. This paper demonstrates the effectiveness of shifting the period by base isolation with two case studies of isolated bridges and a design example.

The design example is a continuation of the Waldo-Hancock Bridge Master of Engineering project completed in 2004 by the author, Andrea Scotti, and Richard Unruh. A side span of the bridge was modeled in SAP 2000 Nonlinear and subjected to the El Centro and Northridge earthquakes that struck California in 1940 and 1996, respectively. Those earthquakes were chosen because there are no recorded earthquakes in the state of Maine. The resulting column shears and deck displacements were compared for no isolation and multiple periods of isolation. It was found that the expected result indicated by the response spectra of the two quakes closely matched the performance of the bridge.

Thesis Supervisor: Jerome J Connor

Title: Professor of Civil and Environmental Engineering



## Table of Contents:

1.	Introduction .....	9
2.	Earthquakes .....	10
2.1.	Introduction .....	10
2.2.	Descriptors .....	11
2.3.	Near and Far Field Earthquakes .....	14
2.4.	Material Amplification .....	14
3.	Earthquake Data Organization .....	15
3.1.	Time History .....	15
3.2.	Response Spectra.....	16
4.	Retrofitting Strategies .....	18
4.1.	Base Isolation .....	21
4.1.1.	Lead Rubber Bearings.....	22
4.1.2.	Friction Pendulum Bearings.....	25
4.1.3.	High-Damping Rubber.....	27
5.	Case Studies .....	30
5.1.	Bolu Viaduct .....	30
5.2.	Bai-Ho Bridge .....	32
6.	Design Example .....	34
6.1.	Introduction .....	34
6.2.	Methodology .....	35
6.3.	Selecting the Earthquake.....	37
6.4.	SAP 2000.....	37
6.4.1.	Importing the Earthquake.....	37
6.4.2.	Building the Model.....	38
6.4.3.	NLLINK Function.....	38
6.4.4.	Viewing the Results .....	38
6.5.	Spectra.....	39
6.6.	Results .....	39
6.7.	Northridge Earthquake .....	46
7.	Discussion and Conclusions.....	51



## Table of Figures:

Figure 1: Collapse of a building in Mexico City 1985. The stairwell with a reinforced shear wall is the only part of the structure to survive (courtesy of Key) .....	10
Figure 2: Earth's Tectonic Plates (courtesy of USGS) .....	11
Figure 3: A map of earthquakes from 1963-1988 with Richter Scale magnitudes greater than 5 (courtesy of Keller) .....	12
Figure 4: Slip Types (courtesy of Keller).....	13
Figure 5: The different wave types created by an earthquake. (courtesy of Keller).....	14
Figure 6: Typical Response Spectrum (courtesy of Naeim) .....	17
Figure 7: A single degree of freedom system .....	18
Figure 8: A multiple degree of freedom system subjected to ground motion.....	19
Figure 9: A frame sitting on isolators.....	21
Figure 10: A Lead Rubber Bearing with a lead core and thin rubber slices bonded to steel plates to provide axial capacity (courtesy of Naeim and Kelly) .....	22
Figure 11: A graph of the loss factor of high-damping rubber (Courtesy of JJ Connor)..	25
Figure 12: The concave sliding surface and sliding surface with the slider .....	26
Figure 13: The storage modulus ( $G_s$ ) and loss factor ( $\eta$ ) of high damping rubber.....	29
Figure 14: The isolation system used in the Bolu Viaduct (Courtesy of Roussis et al)....	31
Figure 15: The location of the Bolu Viaduct in Turkey (Courtesy of reference 13).....	31
Figure 16: The location of the Bai-Ho Bridge in Taiwan (Courtesy of reference 15).....	33
Figure 17: The model used to determine the stiffness of the isolator .....	35
Figure 18: The model used in SAP .....	38
Figure 19: The ground acceleration in terms of time of El Centro .....	40
Figure 20: The response of the bridge to El Centro for different periods.....	41
Figure 21: The spectral acceleration of El Centro.....	42
Figure 22: The spectral displacement of El Centro.....	42
Figure 23: Shear in the columns as a function of the period of the bridge .....	43
Figure 24: The time history of the shear in the piers in the non-isolated case.....	44
Figure 25: The shear in the piers in the case of a period of 4 seconds. The magnitude of the vertical scale is the same as the non-isolated bridge shown in Figure 24 .....	45
Figure 26: The shear in the piers in the case of a period of 4 seconds zoomed in.....	45
Figure 27: The spectral acceleration of the Northridge Earthquake .....	46
Figure 28: The spectral velocity of the Northridge Earthquake.....	47
Figure 29: The spectral displacement of the Northridge Earthquake.....	47
Figure 30: The displacement of the bridge subjected to the Northridge Earthquake and isolated to a period of 1.75 seconds .....	48
Figure 31: The displacement of the bridge subjected to the Northridge Earthquake and isolated to a period of 2 seconds .....	49
Figure 32: The displacement of the bridge subjected to the Northridge Earthquake and isolated to a period of 3 seconds .....	50
Figure 33: The displacement of the bridge subjected to the Northridge Earthquake and isolated to a period of 4 seconds .....	50





# 1. Introduction

There has been a wave of seismic retrofit in the United States in recent years. This new seismic awareness can be traced back to the magnitude 6.7 Northridge Earthquake that struck the Los Angeles area in 1994. Northridge exposed the weakness of the seismic design philosophy when it caused \$40 billion dollars in damage due mostly to the failure of rigid moment frames and bridge supports.

Before undertaking a seismic retrofit it is important for designers to investigate the characteristics of the region. Collisions and slips between tectonic plates cause earthquakes. When the slip along a fault occurs seismic waves with different characteristics and velocities propagate from the site. This phenomenon gives rise to two earthquake classifications. When the city is close to the quake it is termed a near-field quake. An earthquake with an epicenter far away from the point of reference is called a far-field quake. Ground motion near near-field events is much more complex than far-field motion due to the differential wave propagation speeds. High frequency waves tend to die out quickly, further reducing the complexity of the ground motion in a far-field earthquake. Near-field quakes focused deep in the ground and far-field quakes can be further intensified by soil amplification. Finally, seismic designers should know the reoccurrence rates of earthquakes in the region in question.

An important tool for seismic engineers is the response spectrum. The response spectrum graphically shows the response of structures of different periods to the earthquake. They are particularly useful when using base isolation to retrofit the structure. Base isolation is a method of lengthening the period of the structure by adding soft elements to the base of the structure. Other isolation methods depend on strengthening various structural elements. The advantages of base isolation include significantly reducing the shear in the columns and the ability to considerably shift the period. The theory behind base isolation for retrofitting is also easily applied to isolating new structures.

This paper outlines the theory behind base isolation and applies it to an approach span of the Waldo-Hancock Bridge redesign masters of engineering project. A simple

back-of-the-envelope calculation was done to calculate the isolator stiffness necessary to achieve different periods for the approach. Then a model was created in the finite element program SAP 2000 Nonlinear from which the actual isolator stiffness required to attain each period was determined. The results of the models demonstrate the importance of a thorough investigation of the response spectrum of characteristic earthquakes of the region.

## 2. Earthquakes

### 2.1. Introduction

The outer layer of the Earth, the lithosphere, is broken into seven major tectonic plates (Figure 2) ranging from 40 to 100 kilometers in thickness. These plates are in constant motion, floating on the plastic asthenosphere, which is the uppermost layer of the mantle. Each plate moves in roughly the same direction at roughly the same rate, from one to fifteen centimeters a year [1]. As a point of reference that is about as fast as the human fingernails grow. However, the movement rate and direction of the all the plates is not the *exactly* same. The differential movement causes divisions and collisions between plates. When two plates slide relative to each other the seismic energy created can be enormous. An earthquake that hit Mexico City in 1985 destroyed many buildings and injured thousands of people (Figure 1).

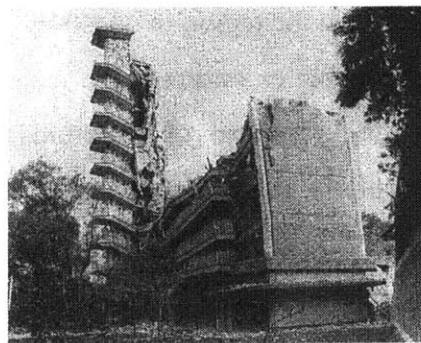


**Figure 1: Collapse of a building in Mexico City 1985. The stairwell with a reinforced shear wall is the only part of the structure to survive (courtesy of Key)**

## 2.2. Descriptors

As the plates move relative to each other there are three kinds of boundary zones formed: divergent, convergent, and transform zones [1]. The majority of earthquakes and volcanoes occur along the plate boundaries as can be seen in Figure 3. Divergence, which is found mostly in the oceans, occurs when two plates are moving away from each other. As gaps open up lava exposed to the ocean cools and solidifies, creating new lithosphere. Divergence is not of much concern to earthquake engineers. The second type of zone is convergence. This is when one plate 'dives' under another plate as the two meet. If the density of the two plates is less than that of granite then instead of one plate diving under the other they collide (continental-collision) forming towering mountain ranges such as the Himalayans. Quakes in this zone are referred to as dip-slips (Figure 4). The final zone is of the most interest to earthquake engineers, the transform zone. In a transform zone one plate rubs against the other. The San Andreas

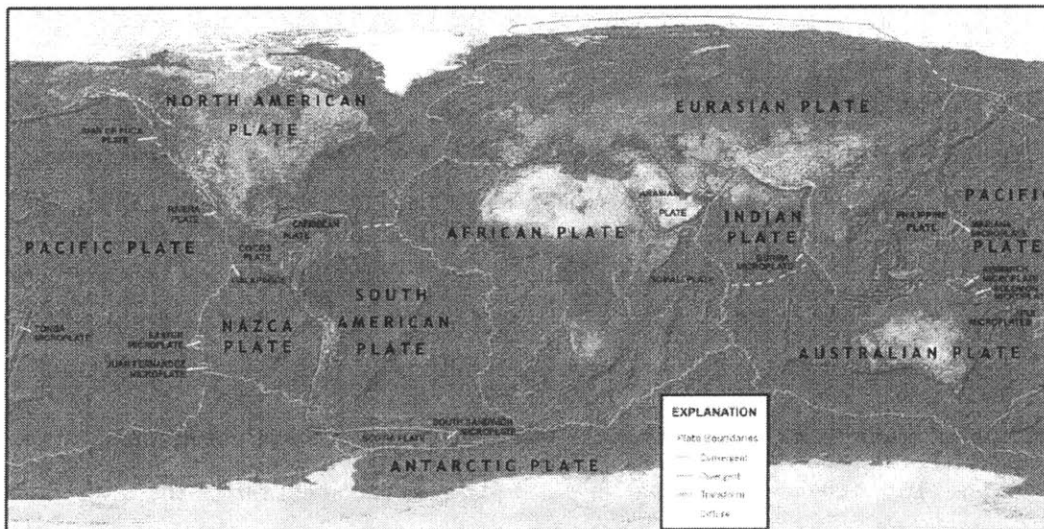
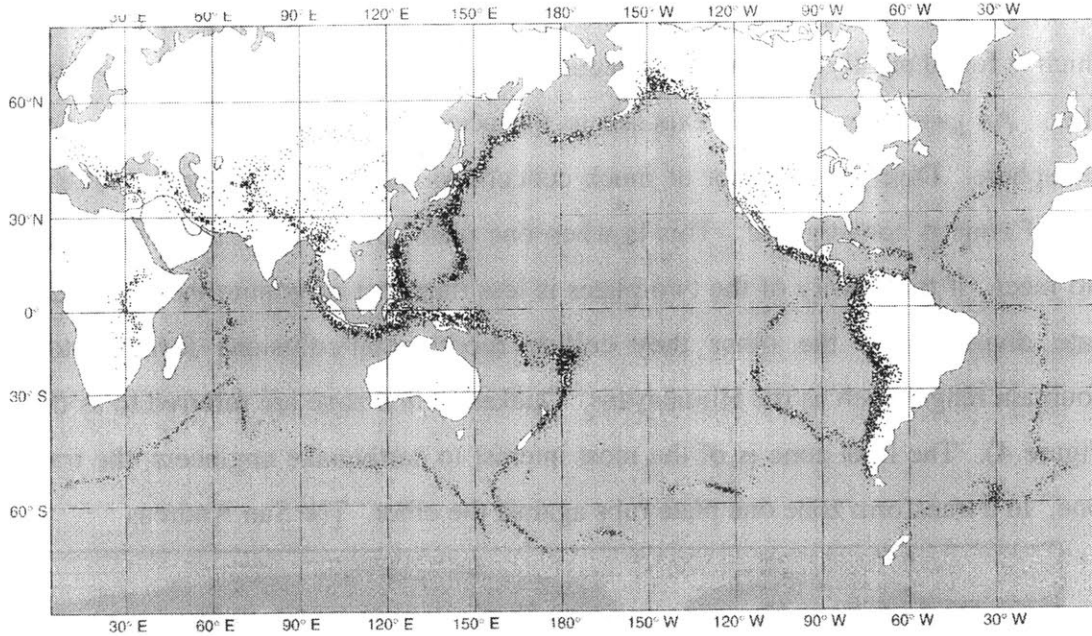


Figure 2: Earth's Tectonic Plates (courtesy of USGS)

Fault in California is of this type. Picture two rough boards being rubbed together slowly. At first the friction keeps the boards stuck to each other. However, as the stress increases the protrusions eventually give way and the boards suddenly slide apart. This is called a lateral slip.

The most well-known earthquake descriptor is the quake magnitude, which is measured on the Richter Scale. The Richter Scale is a measure of the maximum amplitude of seismic waves at a distance of 100 km from the epicenter [1].



**Figure 3: A map of earthquakes from 1963-1988 with Richter Scale magnitudes greater than 5 (courtesy of Keller)**

It is arranged logarithmically, which means that there is a ten times increase in amplitude from magnitude 5 to magnitude 6 and a 32 times increase in power for each unit. Magnitudes of less than 5.5 generally do not have a significant effect on bridges.

The next step in describing an earthquake is the location of the slip. When an earthquake occurs the media reports the epicenter of the quake. Epicenter, however, only locates the quake in two dimensions, on the surface of the earth. The three dimensional location of an earthquake is called the focus.

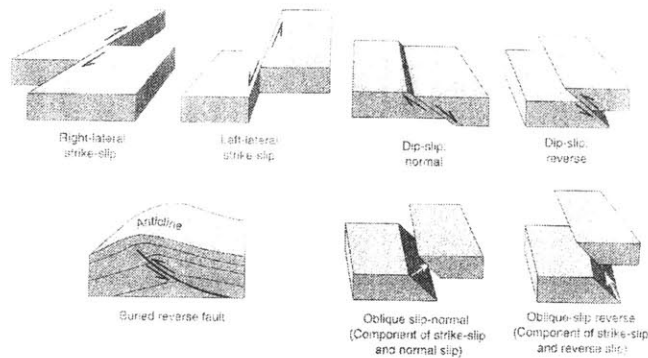


**Figure 4: Slip Types (courtesy of Keller)**

The depth of the earthquake has a major influence on the response felt by buildings on the surface of the Earth. For instance, the Northridge Earthquake, which hit California in 1994, occurred at a depth of 18 km causing \$40 billion in damage. The Nisqually quake, which hit Seattle Washington in 2001 had a focus three times deeper and only caused \$2 billion of damage. Both quakes were very similar in magnitude, 6.7 and 6.8 respectively. The mechanics of a deep earthquake are different than those of a shallow quake because of the different seismic waves created by a slip and because of material amplification [1].

There are two categories of seismic waves: body and surface waves, each with two subcategories. Body waves travel within the Earth. There are two types of body waves, primary waves or P waves and secondary waves, S waves. P waves are the faster of the two, traveling approximately 5.5 km/s through rock. They create pressure in the direction of wave propagation like a worm contracting and expanding as it moves (Figure 5). S waves travel about half as fast P waves, approximately 3 km/s. They produce shearing in the rock normal to the line of propagation. Although S waves may some day be used to detect earthquakes at a distance from major cities they are not the major cause of damage to structures on the surface of the Earth. Body waves have a vast range of frequencies but because the higher frequencies tend to die out quickly body waves generally range from 2 to 0.05 second periods. Surface waves travel slower than body waves. They come in two varieties, Love Waves and Rayleigh Waves. Love Waves, the faster of the two, cause horizontal ground motion [1]. Rayleigh Waves are rolling waves

much like ocean waves [Design Codes]. Surface waves have periods greater than 1 second [1].

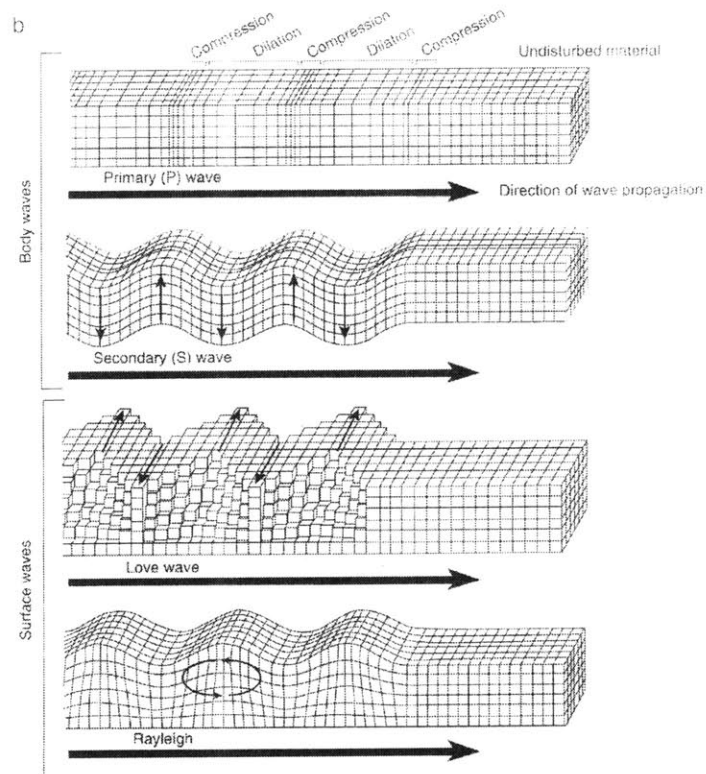


Figure 5: The different wave types created by an earthquake. (courtesy of Keller)

### 2.3. Near and Far Field Earthquakes

Due to the different speeds at which they travel, waves tend to separate into distinct groups as they travel away from the epicenter of the fault slip. In a near field quake there is no time for the waves to segregate causing structures to feel very complex earth motions. The direction of rupture of the fault can also cause energy to be directed in a particular direction for near-field earthquakes. In the direction normal to the fault line there are large long-period spectral components. Large short-period components develop in the direction parallel to the fault. There are also long-duration pulses of ground displacement and high peak ground velocities in near-field quakes [5].

### 2.4. Material Amplification

There is also the danger of material amplification in both near-field and far-field quakes. The presence of unconsolidated sediments can amplify seismic power more than five times [1]. Material amplification is more of a concern in far field quakes however.

The case of the Mexico City Earthquake of 1985 is an example of the effect that material amplification can have on seismic power. Mexico City is built on the bed of an ancient lake. The period of the soil is estimated to be approximately 2 seconds. In 1985 an earthquake occurred with an epicenter 250 miles offshore. Although seismic waves contain a great variety of frequencies, the highest frequencies generally die out quickly, leaving the bulk of frequencies between 0.5 Hz and 20 Hz. That is equivalent to periods from 2 to 0.05 seconds. Therefore when the waves reached Mexico City they excited the soil resulting in a wave power amplification of four to five times, causing massive damage to structures six to sixteen stories in height [1]. Generally the fundamental (resonant) period of a building is approximately equal to the number of stories divided by ten. A typical sixteen-story building has a period of 1.6 seconds.

### **3. Earthquake Data Organization**

Earthquake energy output data has historically been organized for seismic design by three methods: frequency domain, time history, and response spectra. Because of the geology and geography of a site, earthquakes in the same region generally share certain characteristics [1]. Therefore, when designing a structure engineers need to know the time interval of reoccurrence of different magnitude seismic events, the history of the acceleration, and the frequencies among other things [2].

#### **3.1. Time History**

Probably the most common way of displaying an earthquake's characteristics is the time history plot [3]. Time history has some advantages, namely availability for non-linear (multiple degree of freedom) structures, display of time history response of input energy, and possibility of expressing the input energy rate. A time history plot can display the displacements, velocities, or accelerations imposed on the ground as a function of time. For design purposes the peak values of each function are used, Peak Ground Displacement (PGD), Peak Ground Velocity (PGV), and Peak Ground Acceleration (PGA). PGA is the value most extensively used in the design codes. However, the correlation between PGA and structural damage is being questioned. Naeim and Kelly [6] explain that acceleration is generally associated with high

frequencies, and therefore low periods, which do not affect isolated structures due to longer periods created by isolation. They recommend the use of PGV as the primary design value. Karim and Yamazaki [7] disagree however. In their study to determine the fragility curve for a structure they used a seismic intensity index created by the Japan Meteorological Agency, which uses a combination of PGD, time duration of strong motion, spectrum intensity, and spectral characteristics to define seismic input energy. Fragility curves show the relationship between the probability of structural damage and ground motion.

### 3.2. Response Spectra

The seismic design codes emphasize the use of Response Spectra. Response Spectra display the response of a single degree of freedom (SdoF) system to an earthquake. A spectral plot shows the relative displacement, relative velocity, and absolute acceleration as a function of period as seen in Figure 6 [6]. Relative values for displacement and velocity are used because member forces are proportional to relative displacement and velocity using Hook's Law. Absolute acceleration is used because Newton's Law states that the inertia force is equal to absolute acceleration multiplied by the mass of the object. As the Figure 6 shows there are peaks and troughs in the graph. This is due to the fact that this is a spectrograph of a single earthquake. In order to generalize the spectrum for a characteristic quake a number of earthquakes must be averaged together to form a Smoothed Response Spectrum. The following equations are used to create Response Spectra [8].

$$SD = u(t) = \frac{1}{\omega} \int_0^t \ddot{u}_g(\tau) e^{-\xi\omega(t-\tau)} \sin \omega(t-\tau) d\tau$$

$$SV = \dot{u}(t) = -\int_0^t \ddot{u}_g(\tau) e^{-\xi\omega(t-\tau)} \cos \omega(t-\tau) d\tau + \xi \int_0^t \frac{\ddot{u}_g(\tau) \omega (1 - 2\xi^2)}{\sqrt{1 - \xi^2}} e^{-\xi\omega(t-\tau)} * \sin \omega(t-\tau) d\tau$$

$$SA = \ddot{u}(t) = 2\xi\omega \int_0^t \ddot{u}_g(\tau) e^{-\xi\omega(t-\tau)} \cos \omega(t-\tau) d\tau + \int_0^t \frac{\ddot{u}_g(\tau) \omega (1 - 2\xi^2)}{\sqrt{1 - \xi^2}} e^{-\xi\omega(t-\tau)} \sin \omega(t-\tau) d\tau$$



These equations can be simplified if  $\xi$  is small. Often structures, even ones designed for additional damping, have values of  $\xi$  less than ten percent. In that case we have the following approximations.

$$SV \approx \dot{u}(t) = -\int_0^t \ddot{u}_g(\tau) e^{-\xi\omega(t-\tau)} \cos \varpi(t-\tau) d\tau$$

$$SA \approx \ddot{u}(t) = \int_0^t \ddot{u}_g(\tau) \omega e^{-\xi\omega(t-\tau)} \sin \varpi(t-\tau) d\tau$$

Which means that:

$$\text{Pseudoacceleration (PSA)} = \omega * SV = \left(2 \frac{\pi}{T}\right)^2 * SD$$

$$\text{Pseudovelocity (PSV)} = \omega * SD = 2 \frac{\pi}{T} * SD$$

Response Spectra are useful because they show the effect changing the fundamental period has on the response of a structure.

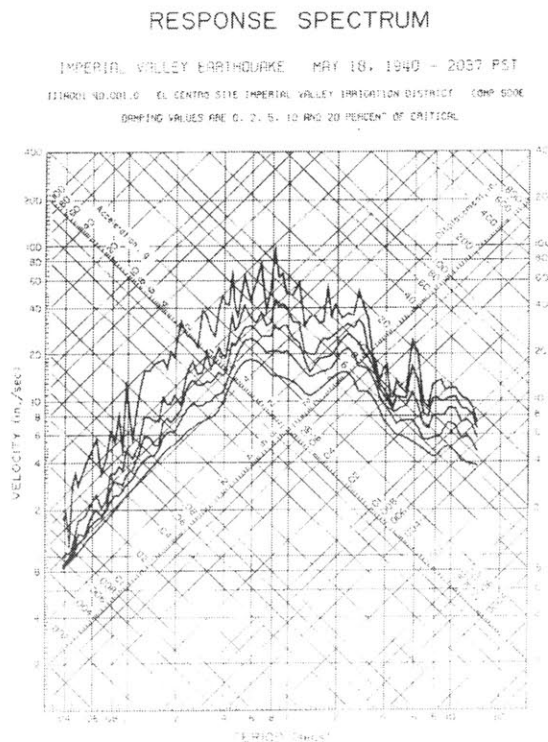


Figure 6: Typical Response Spectrum (courtesy of Naeim)

## 4. Retrofitting Strategies

There are three fundamental ways that structures can respond to the energy input by a seismic event. Structures can absorb, dissipate, or avoid the input energy.

First, think of the structure as a solid block of granite heavy enough to remain stationary during a seismic event. After construction Sensor A is attached to the top of the block, Sensor B is attached to the midpoint, and Sensor C to the ground nearby. When the earthquake occurs the block moves exactly with the ground. In other words, all three sensors display the same displacements, velocities, and accelerations at the same times (Figure 7).

This solid block is a single degree of freedom (SDOF) system. All locations of the block move like a rigid body. For a structure to react this way it would have to be built with members and connections that are very stiff. The structure would be strong enough to withstand the input energy. There are some problems with this design methodology. Firstly, it is impossible to design and construct a building over a few stories or a bridge that would work as a SDOF. Secondly, assuming it is possible, the cost of doing so would be enormous.

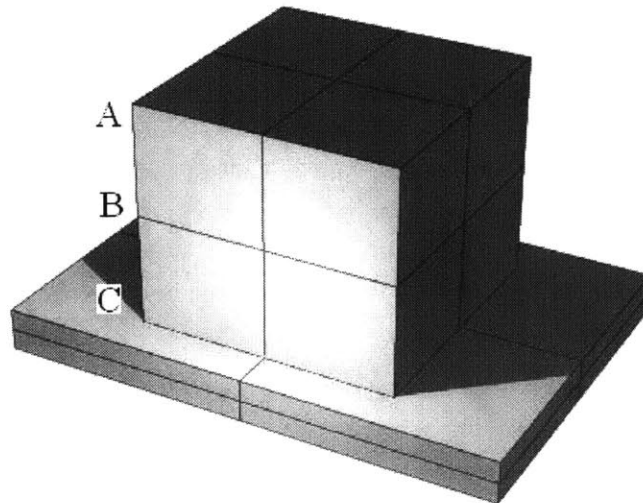
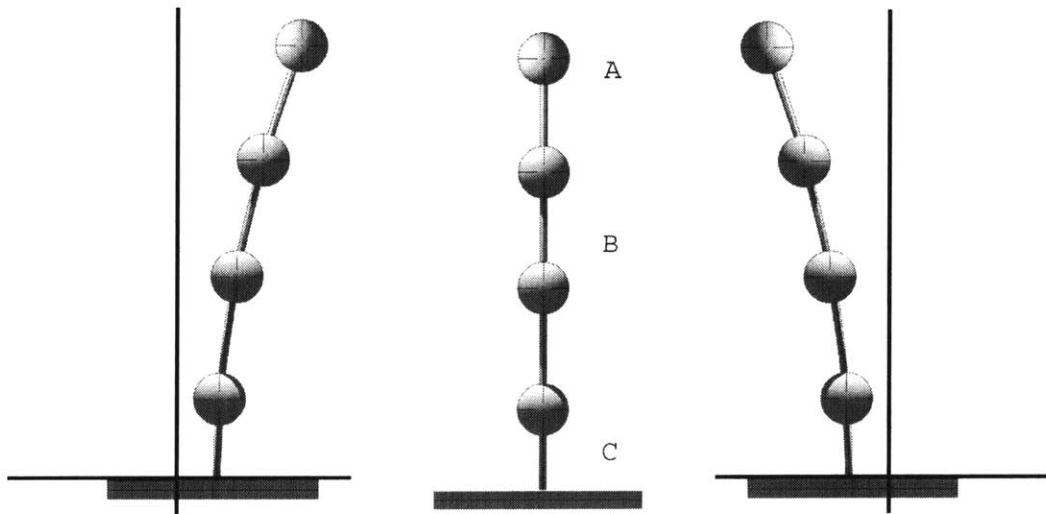


Figure 7: A single degree of freedom system

Thirdly, if an earthquake of a greater magnitude than the design quake hits the structure it will undergo deformation of the members and failure of the connections. In the Northridge Earthquake 12,500 buildings sustained moderate to severe damage while 7,000 more were deemed unsafe. The reason for much of the damage was due to the use of moment frames in buildings [9]. When the seismic energy exceeded the capacity of the moment frame the joints failed. Finally, there are safety issues associated with this design methodology. Although the structure will move with the ground motion things inside the building will not. Bookshelves, filing cabinets, computers, sophisticated machinery, and people would all be thrown back and forth by the quake.

Next, think of the structure as a number of masses connected by springs, which are lumped at points along the structure (Figure 8). Each mass is able to move independently of the others. This is called a multiple degree of freedom (MDOF) system. A MDOF system reacts differently than a SDOF system to an earthquake. Again Sensors A, B, and C are attached to the top, middle, and ground respectively. When the structure is seismically excited the three sensors do not all read the same displacements, velocities, and accelerations. Sensor B feels less maximum displacement, velocity, and acceleration than the ground and Sensor A feels less than B.



**Figure 8: A multiple degree of freedom system subjected to ground motion**

This system has two methods of dealing with the energy input by the seismic event: it can absorb the energy with strength and it can dissipate some of the energy with

dampers. Dissipation is available in the MDOF because of the differential displacement between stories. Viscous or hysteretic dampers can be installed as a diagonal brace in a frame. In viscous damping the damping force is equivalent to the time rate of change of the displacement [8]. The function of a viscous damper is analogous to the way a revolving door works. If the door is pushed gently it begins to revolve. However, if the door is pushed very hard it does not move. That is because the velocity of the door is higher in the second case.

Hysteretic damping occurs when metals yield. The damping is a function of the yield strength and ductility of the material. Ductility,  $\mu$ , is the ratio of absolute displacement to the displacement at yielding. From a safety point of view hysteretic damping caused by structural members yielding is a good thing. It dissipates energy and increases the damping of the structure. However, from a cost perspective yielding of structural members is negative. Repairing the damage caused is extremely expensive. It is possible to dissipate energy before the structural steel can yield if a material with a lower yielding strength is used, such as lead or low quality steel [8].

The final method of coping with the input energy from an earthquake is to avoid the energy. The effect of energy input in the system is magnified when the frequency of the input energy is equal to the fundamental frequency of the system. This effect is called resonance. The fundamental frequency of the system is equal to the square root of the stiffness divided by the total mass [8].

$$\omega = \sqrt{\frac{k}{m}}$$

Although buildings have many modes of vibration the first mode is generally the most important when designing structures for dynamic excitation. By definition the first mode always has the lowest frequency of vibration and it also usually has the greatest percentage of mass participation. In general structural engineers deal with periods rather than frequencies. Frequencies can be converted to a period by dividing the frequency (in radians per second) by 2 Pi.

$$T = \frac{2\pi}{\omega} = \frac{2\pi}{\sqrt{\frac{k}{m}}}$$

In the case of bridges shifting the period to above 0.6 seconds considerably reduces the peak spectral acceleration as can be seen in Figure 6 [10]. There are two methods of shifting the period sufficiently to avoid the major portion of the input energy. First increasing the mass of the system will raise its period. This solution does not seem like the best solution. Adding mass would increase the dead weight of the building, waste space and material, and is not a very elegant solution. Secondly reducing the total stiffness of the system will increase the period. Decreasing the stiffness of the columns would increase the period, but at the risk of reducing the strength of the system. Isolating the base of the structure on springs can also reduce the total system stiffness (Figure 9).

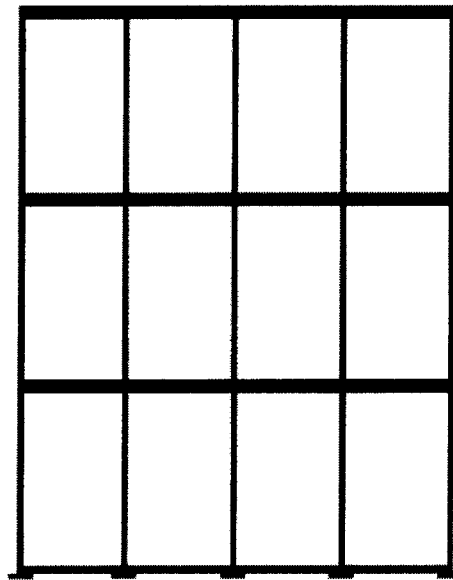


**Figure 9: A frame sitting on isolators**

#### **4.1. Base Isolation**

Base isolation systems must not be too soft. They must provide sufficient strength under low-power periodic excitations such as wind but must isolate the bridge and

dissipate energy under extreme excitations such as an earthquake. There also seems to be an optimal stiffness, which significantly reduces acceleration of the structure while minimizing the displacement experienced by the isolator. Very large displacements are undesirable because they can lead to isolator instability and insufficient restoring forces [5, 6].

There are four isolation systems generally used to isolate bridges: Lead Rubber Bearings (LRB), Elastomeric Bearings, and High-Damping Rubber, Friction Pendulum Bearings (FPB) [5]. The first three systems use high-damping, low stiffness materials to dissipate energy and increase the period of the structure.

#### 4.1.1. Lead Rubber Bearings

Lead rubber bearings (LRB) were invented in New Zealand in 1962 [6]. LRB evolved from the idea of using thick chunks of rubber to achieve a perfectly elastic behavior, known as elastomeric isolators. However, when rubber is axially loaded it bulges, significantly reducing the axial capacity of the bearing. To solve this problem thin slices of rubber are bonded to steel plates.

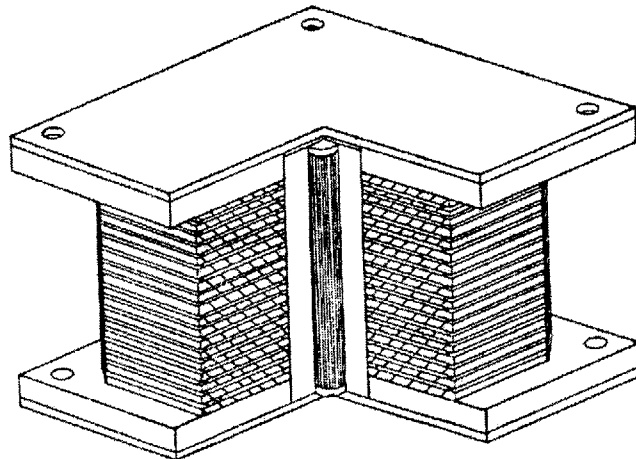


**Figure 10: A Lead Rubber Bearing with a lead core and thin rubber slices bonded to steel plates to provide axial capacity (courtesy of Naeim and Kelly)**

This solution provides a high vertical stiffness while leaving the horizontal stiffness unaffected [6]. These simple rubber bearings are easy to manufacture, inexpensive, and easy to model. However, they have two major drawbacks. First, they provide only two

to three percent damping and therefore require additional viscous or hysteretic dampers to be installed in the building. Viscous dampers obstruct the diagonals of frames and are expensive. Second, rubber's stiffness and damping capacity are dependent on environmental temperature. Temperatures below  $-40^{\circ}\text{C}$  can cause the rubber to glassify and a change of  $60^{\circ}\text{C}$  can result in a 30% change in stiffness [10].

The LRB is an elegant and inexpensive solution to that problem. Lead rubber bearings increase the damping capacity of the simple rubber bearing without any additional damping require in the system by incorporating hysteretic damping in the damper itself. The center of the LRB is drilled out and filled with a lead core, which serves two functions. It increases the horizontal stiffness of the system under stresses lower than the yield stress of lead, and provides additional hysteretic damping when stressed beyond its yield stress (Figure 10). That means that under low-force horizontal loadings such as wind the building will act as a non-isolated building. But under extreme loadings like a seismic event the lead will yield providing additional damping, and therefore dissipating energy, while the rubber reduces the stiffness of the system at the base, shifting the period out of the power zone of the quake [6].

Stiffness Equations [8]:

$$\mu = \frac{u}{u_y}$$

$$k_s = k_1 + \frac{k_2}{\mu}$$

Where:

$\mu$  = ductility ratio

$k_1$  = the stiffness of the rubber

$k_2$  = the stiffness of the lead core

$k_s$  = the secant stiffness

A reasonable value for  $k_2$  is ten times that of  $k_1$ .

$$k_s = 1.1k_1$$

In order to find the average value of the secant stiffness it is necessary to use the least squares approach treating  $k_s$  as a function of strain and frequency [8].

$$k_{eq} = \frac{1}{N} \sum_{i=1}^N k_s(\mu_i, \Omega_i)$$

Where:

N = number of data sets

Damping:

The damping provided by the system of the lead rubber bearing is a function of the equivalent stiffness, a material property called the loss factor ( $\tilde{\eta}$ ) shown in Figure 11, and the frequency of the excitation. Rubber loss factor is dependent on the frequency of the excitation and the temperature of the environment. It varies inversely to temperature and proportionally to frequency. The lower the temperature and higher the frequency of excitation the greater value of the loss factor [8].

$$\tilde{\eta} = \frac{4(\mu - 1)k_2}{k_s \mu^2 \pi} + \eta \frac{k_1}{k_s}$$

For information on the derivation of  $\tilde{\eta}$  see *Introduction to Structural Motion Control* by JJ Connor.

Using:  $k_s = 1.1k_1$  we can derive a typical value for  $\tilde{\eta}$ .

$$\tilde{\eta} = \frac{4}{11\pi} + \frac{0.1}{0.11} \eta = 0.12 + 0.909\eta$$

Where  $\eta$  can be taken from:



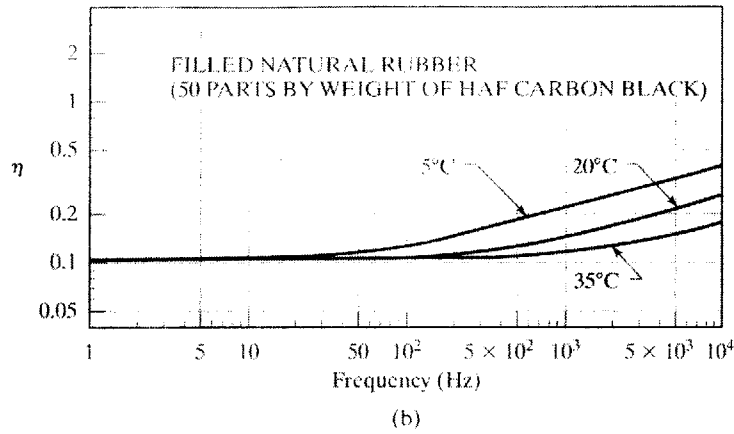


**Figure 11: A graph of the loss factor of high-damping rubber (Courtesy of JJ Connor)**

Finally, the damping derived using least squares:

$$c_{eq} = \frac{1}{N} \sum_{i=1}^N \frac{k_s(\mu_i \Omega_i) \tilde{\eta}(\mu_i \Omega_i)}{\Omega_i}$$

### 4.1.2. Friction Pendulum Bearings

Friction pendulum bearings (FPB), also commonly referred to as sliding friction bearings, consist of a concave spherical surface and a slider. The slider acts like a pendulum as it slides along the curved surface, isolating the structure and dissipating energy by friction. It is coated with a low friction material. The stiffness and period of the pendulum are determined by selecting the proper radius of curvature. One benefit of the FPB is the fact that the weight of the bridge acts as a restoring force returning the structure to its original position at the end of the excitation [10].

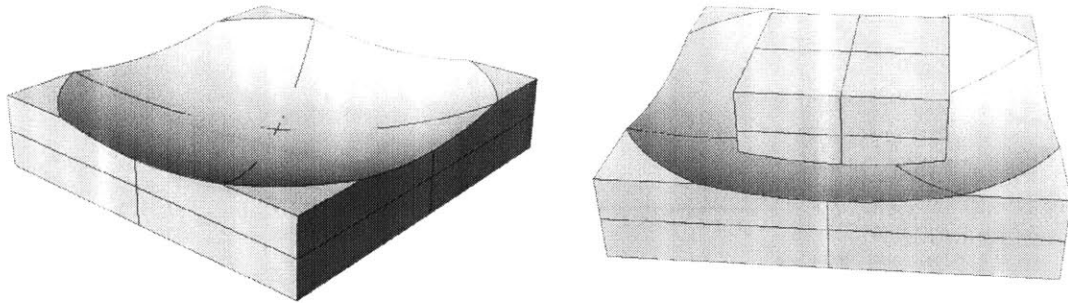


**Figure 12: The concave sliding surface and sliding surface with the slider**

The horizontal force at any displacement [6]:

$$F = \mu W + \frac{W}{R} D$$

Where:

$\mu$  = coefficient of friction

$W$  = weight of the structure over the tributary area

$R$  = radius of curvature

$D$  = displacement

The effective stiffness of the friction pendulum bearing:

$$K_{eq} = \frac{W}{R} + \frac{\mu W}{D}$$

The period of the FPB [10]:

$$T = 2\pi \sqrt{\frac{R}{g}}$$

Where:

$g$  = gravity

Finally, the damping provided by the bearing [6]:

$$c = \frac{2\mu}{\pi \left( \frac{D}{R} + \mu \right)}$$

Now the equations can be rearranged to give a better perspective of the geometry of the system.

$$R = \frac{gT^2}{(2\pi)^2} \approx \frac{1}{4}T^2 \text{ meters}$$

And an approximate value of the vertical displacement:

$$\delta_v \approx \frac{D^2}{2R}$$

To shift the period of bridge out of danger range a period of 1.5 seconds is required. To achieve this period a radius of 0.56 meters is needed. If the structure displaces half of a meter then the corresponding vertical displacement is 0.22 meters.

### 4.1.3. High-Damping Rubber

Natural rubber with a high enough damping coefficient to be useful for isolation situations was invented in 1982 by the Malaysian Rubber Producers' Research Association of the United Kingdom. Rubber is modified by adding extrafine carbon blocks, oils, and other priority fillers. Damping that can be obtained ranges from 10 to 20% of critical at around 100% shear strains. The shear modulus decreases as the shear strain increases [6]. The material is non-linear for shear strains below 20%. It is approximately linear for shear strains from 20 to 120%. At large strains the rubber undergoes strain crystallization, developing a high shear modulus and an increased energy dissipation capacity.

High-damping rubber is a viscoelastic material. That means that it performs like neither a viscous damper nor an elastic damper [6]. The displacement of the high-damping rubber bearing under harmonic excitation:

$$u = \hat{u} \sin(\Omega t)$$

Where:

$\hat{u}$  is the maximum amplitude of displacement

$\Omega$  is the frequency

The resulting force in the rubber:

$$F = f_d G_s \hat{u} [\sin(\Omega t) + \eta \cos(\Omega t)]$$

Where:

$G_s$  is the storage modulus a material property shown in Figure 13

$\eta$  is the loss factor a material property

$$f_d = \frac{A}{h}$$

Where:

$A$  is the area of the top or bottom

$h$  is the height of the section

Using the standard form of the force equation:

$$F = k_{eq} u + c_{eq} \dot{u}$$

And finding the equivalent stiffness and equivalent damping using the least squares approach.

$$k_{eq} = f_d \left[ \frac{1}{N} \sum_{i=1}^N G_s(\Omega_i) \right]$$

$$c_{eq} = \alpha k_{eq}$$

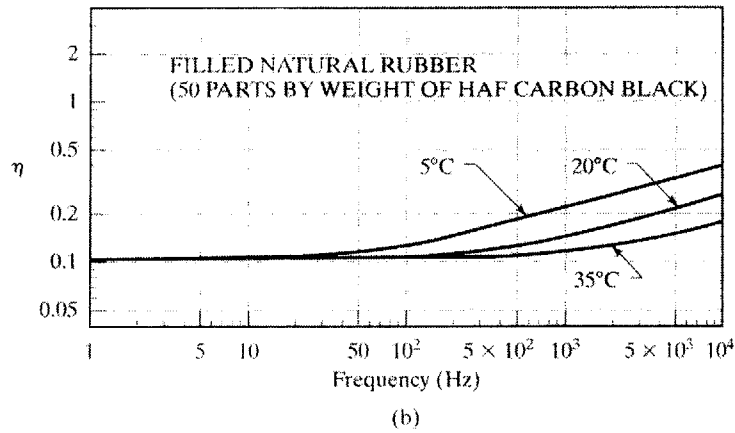
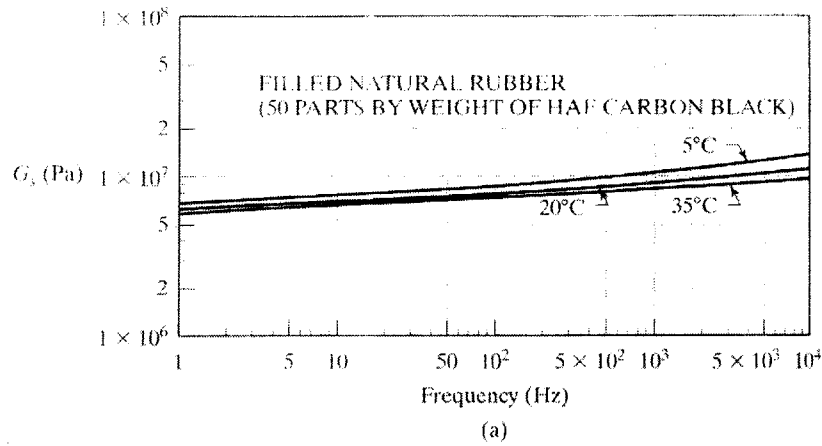


**Figure 13: The storage modulus ( $G_s$ ) and loss factor ( $\eta$ ) of high damping rubber**

$$\alpha = \frac{\sum_{i=1}^N \left( \frac{G_s \eta}{\Omega} \right)_i}{\sum_{i=1}^N G_s(\Omega_i)}$$

Recognizing that in frequencies less than 20 Hz the values for  $G_s$  and  $h$  are relatively constant, and the frequencies we are worried about are less than 20 Hz, the equations above can be simplified to:

$$k_{eq} = f_d G_s$$

$$\alpha = \frac{\eta}{2\pi} T_{ave}$$

Where:

$T_{ave}$  is the average period for the excitation

$$G_s = 4.8 \times 10^5 \text{ Pa}$$

$$\eta = 0.022$$

## 5. Case Studies

The following section attempts to demonstrate the effectiveness of base isolation for protecting bridges from seismic excitation. The first bridge, the Bolu Viaduct in Turkey [11], was in the final stages of construction when it experienced an earthquake. Sensors placed on the deck of the Bai-Ho Bridge in Taiwan [12] gave insight into the performance of the bridge when it experienced a seismic event not long after construction.

### 5.1. *Bolu Viaduct*

The Bolu Viaduct [11] is located in northern-central Turkey in the province of Bolu marked with a red 'x' in Figure 15. It is 2.3 km long and consists of 59 spans supported by 58 piers. The bridge is isolated with sliding pot bearings with stainless steel-polytetrafluoroethylene sliding surfaces. For additional damping hysteretic dampers were used. They consist of a dual level spiral array of C shaped steel pieces Figure 14. The inner ring is connected to the substructure while the outer ring connects to the superstructure. At the expansion joints the members were connected with cable restrainers. Because Turkey is an affiliate AASHTO state the designers used the 1991 AASHTO Guide Specifications for Seismic Isolation Design and some of their own guidelines.

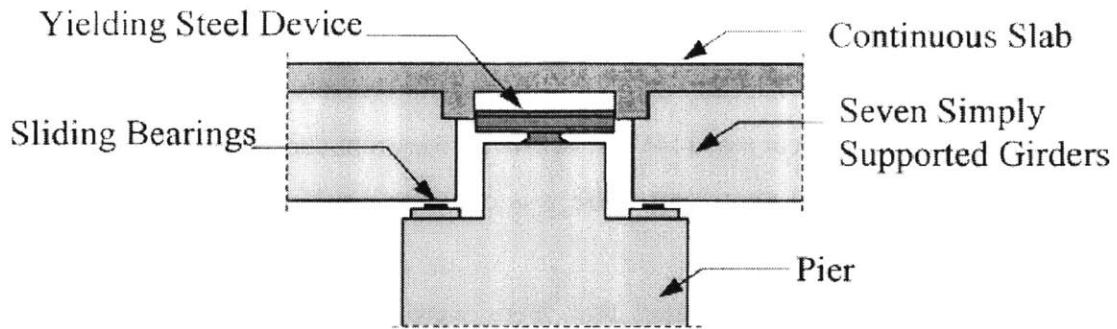


**Figure 14: The isolation system used in the Bolu Viaduct (Courtesy of Roussis et al)**

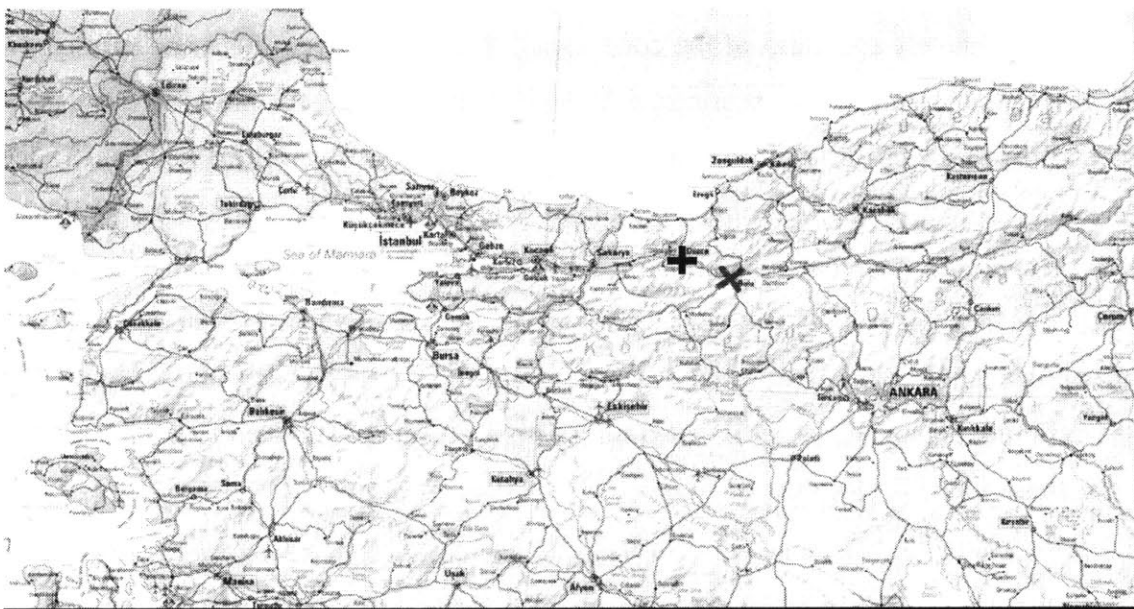


**Figure 15: The location of the Bolu Viaduct in Turkey (Courtesy of reference 13)**

On November 12, 1999 an earthquake of magnitude 7.2 rocked Turkey. The town of Duzce, marked with a blue cross in Figure 15, within the Bolu province was the epicenter of the quake. A right lateral strike-slip rupture along 40 km of the fault caused the Duzce quake. The estimated peak ground acceleration was over  $1g$  [13]. Therefore it is evident the Bolu Viaduct felt a complex near-field seismic event characterized by a broad band of frequencies [1]. The quake resulted in more than a thousand deaths and extensive damage to many buildings, a tunnel, another bridge, and the Bolu Viaduct. In fact the bridge suffered a complete failure of the isolation system and was close to collapse [11].

Because the earthquake crossed the viaduct, near pier 46, it caused a permanent displacement along the ground. As a result the superstructure experienced a permanent displacement of one meter laterally and half a meter transversely. Pier 46 rotated about 12 degrees around its vertical axis [14]. At nearly all locations the sliding bearing fell off the piers. In the west end abutments there was concrete crushing caused by pounding from the bridge deck [web].

An investigation demonstrated that there were significant problems with the isolation design of the Bolu Viaduct. The bridge did not meet the design requirements of the AASHTO codes. Of concern was the fact that the design displacement (320 mm) is only approximately one third of the code value (800 mm). Even more concerning was the fact that the sliding pot bearings only had a capacity of 210 mm. So even under displacements the bridge was designed for the sliding pot bearings still would have failed. Another problem is the restoring force of the bridge is too low. Under the new 1999 AASHTO design guidelines the bridge must be analyzed using a three-dimensional non-linear dynamic analysis. The codes require the use of three time histories scaled to appropriate values. However, even a system designed to AASHTO standards would have still suffered damage because the maximum displacement is estimated to have been near 1.4 meters [11].

## **5.2. *Bai-Ho Bridge***

The Bai-Ho Bridge [12] is located in southwestern Taiwan, marked with a red 'x' in Figure 16. It is a three span bridge stretching 145 meters. When it was completed in 1999 it was the first seismically isolated bridge in Taiwan. The isolator system consists of two parts. Above each pier it has a pair of rectangular lead rubber bearings measuring 1.52m by 1.25m and 0.25m deep. Polytetrafluoroethylene bearings, located at the abutments, carry the vertical weight and add damping to the system. The Bai-Ho Bridge is also outfitted with 24 accelerometers located along the deck, piers, and ground nearby [12].

Just a few days after the monitoring system went into operation Taiwan was hit by the Gia-I earthquake of magnitude 6.4 [14]. The epicenter of this quake was 25 km away



at 23.51°N and 120.40°E. The bridge suffered no damage during the quake because the dominant frequencies of the earthquake closely matched those identified as dominant frequencies during design (Table 1) [12]. The authors decided that the difference in frequencies of the higher modes is due to non-linearity of the isolators and the effects of the boundary conditions at the abutments. Also of interest are the findings of this study about the boundary conditions at the abutments.

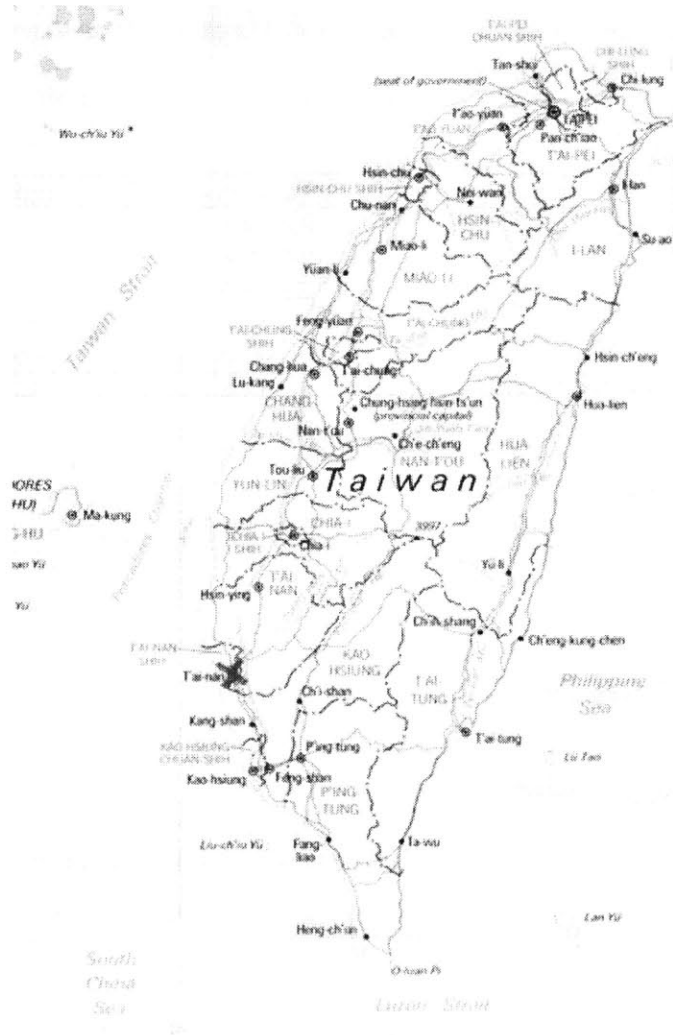


**Figure 16: The location of the Bai-Ho Bridge in Taiwan (Courtesy of reference 15)**

The abutments were designed as ‘hinged ends’ assuming infinite stiffness from the abutments. A model run to test the effects of ‘hinged end’ boundary conditions demonstrated that it lead to higher natural frequencies during the intense phase of the earthquake. This led them to believe that the stiffness of the abutments should not be

infinite. Instead they proposed a model somewhere between a hinged end and free end model, based on horizontal springs. When the stiffness in the springs becomes infinity the horizontal displacement becomes zero and the system acts like a hinged end model. It acts like a free end model when the stiffness is infinite and the displacement is unrestrained [12].

**Table 1: The frequencies of the Bai-Ho Bridge identified in tests and found during an earthquake (Courtesy of Lee et al)**

Ambient Vibration Test									
	Vertical			Tansverse			Longitudinal		
Test 1	1.8	3.2	3.8	2.4	4.2				3.2
Test 2	1.8	3.1	3.8	2.2	2.6				3.1
Test 3	1.8	3.2	3.8	2.2	4.2				3.2
One moving truck test									
	Vertical			Transverse			Longitudinal		
Test 1	1.8	2.3	4.3	2.2	2.6	4.2	1.3	2.8	3.4
Test 2	1.8	2.5	3.8	2.3	3.3	5.5	1.4	2.6	3.4
Test 3	1.8	2.3	4.3	2.2	2.6		1.5		3.5
180-gal scale earthquake									
	Vertical			Transverse			Longitudnal		
10/22/1999	1.8	4.5	10.1	1.3	3.1	12.1	1.1	12.0	

## 6. Design Example

### 6.1. Introduction

In order to better understand the process of base isolation detailed above an example was applied to an approach span of the Waldo-Hancock Bridge in Maine. This is an extension of the Waldo-Hancock Bridge MEng project completed by the author, Andrea Scotti, and Richard Unruh. It was decided that the main span did not require any isolation because it has a fundamental period far beyond the energy spectra of earthquakes.

Basic analysis was completed by hand while a more detailed analysis was obtained by analyzing a simplified bridge model created in the finite element program SAP 2000 Nonlinear. Spectrographs were generated using the program Spectra.

## 6.2. Methodology

Standard bridge isolating behavior was followed by placing lead rubber bearings at the top of the piers, isolating the superstructure from the substructure. A simplified model was created in order to obtain a first approximation of the required stiffness of the isolator. The bridge was modeled as a single degree of freedom system with a lumped mass on a pair of springs Figure 17. The mass calculated as the mass of the deck and the mass of the columns. The stiffness of the column was estimated using the equation of stiffness of a cantilever.

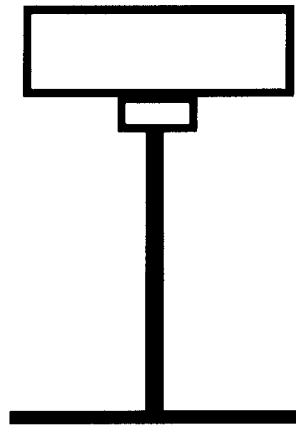


Figure 17: The model used to determine the stiffness of the isolator

$$k_p = \frac{3EI}{L^3}$$

Knowing the stiffness of the pier and the mass of the SdoF system the stiffness of the isolator was calculated by the following process detailed in Structural Motion Control.

The forces are equal at any point in the beam, applying equilibrium:

$$k_b u_b + c_b \dot{u}_b = k u + c \dot{u}$$

Ignoring damping:

$$u_b = \frac{k}{k_b} u$$

The equation of motion of the system is:

$$m(\ddot{u} + \ddot{u}_b) + ku = -m\ddot{u}_g$$

Substituting  $\ddot{u}_b$

$$m\ddot{u}\left(1 + \frac{k}{k_b}\right) + ku = -m\ddot{u}_g$$

Dividing through by m:

$$\ddot{u}\left(1 + \frac{k}{k_b}\right) + \omega^2 u = -\ddot{u}_g$$

Finally:

$$\ddot{u} + \Gamma\omega^2 u = -\Gamma\ddot{u}_g$$

Where:

$$\Gamma = \frac{k_b}{k + k_b}$$

The equivalent frequency:

$$\omega_{eq}^2 = \Gamma\omega^2 = \frac{k_b}{k + k_b} \frac{k}{m}$$

Solving for  $k_b$ :

$$k_b = \frac{\omega^2 m}{1 - \frac{\omega^2 m}{k}}$$

### **6.3. Selecting the Earthquake**

There have been no earthquakes in Maine in recorded history. Therefore it is impossible to generate a smoothed response spectra for past earthquakes. Instead two well-known earthquakes were chosen, El Centro and Northridge. Most of the analysis was done using the El Centro time history, which is a near-field earthquake. Then the results were verified using the response of the bridge to the Northridge quake.

### **6.4. SAP 2000**

The following is a short tutorial on the use of SAP 2000 Nonlinear to generate the response of a structure subjected to a seismic event.

#### **6.4.1. Importing the Earthquake**

Earthquake records can be downloaded from the University of Berkley website [16]. Most earthquake record files are text files (\*.txt files). Open the file in Microsoft Excel in order to determine the number of records and the time step interval of the record. Next, in SAP follow the path “Define: Time History Function” and click on the “Add Function from File” button. Open the earthquake file to be used and enter the number of points per line (usually two, one for time one for acceleration). Then to add a time history case follow the path “Define: Time History Cases: Add new History”. As most records are in percent gravity it is necessary to scale the quake by gravity, in the case of this model  $9.81 \frac{m}{s^2}$ . Also include a modal damping of 2 to 5%. Then input the step size and number of output steps, which were, determined earlier using Excel.

### 6.4.2. Building the Model

The model for this experiment was drawn in AutoCAD, saved as a “.dxf” file, and imported into SAP. The primary model was a simple two bay frame, fixed at the ground. The legs were five meters high and the bays were ten meters wide (Figure 18). The legs were arbitrarily chosen to be square concrete sections two meters wide. Deck properties are the same as the ones determined in the Waldo-Hancock Bridge project.

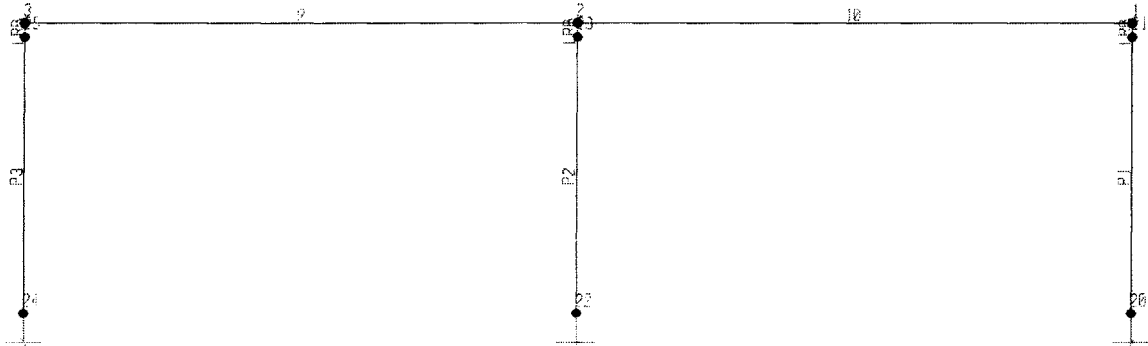


Figure 18: The model used in SAP

### 6.4.3. NLLINK Function

Isolators are modeled in SAP with the NLLINK function. NLLINK were inserted in the bridge by offsetting the deck a quarter of a meter from the top of the piers and then connecting the two joints with “Draw: NLLINK”. Then NLLINK properties were defined (Define: NLLINK) by entering the same stiffness and damping ratio for all six degrees of freedom.

### 6.4.4. Viewing the Results

Once all the properties are defined click “Analyze: Run” or press F5. When the program has finished analyzing the data select the joints and frames of interest and follow the path “Display: Show Time History Traces”. In the case of this project the shear in the piers and the displacement of the deck were considered to be of the greatest interest. In order to determine the direction of greatest displacement and therefore shear a movie showing the response of the bridge in real time was created. Movies can be created by clicking on “File: Create Video: Create Time History Animation Video”. In the case of

this bridge in the El Centro earthquake the greatest displacement occurred in the global Y direction, which coincides with the mode shape of the first mode.

To see the results of the shear in the piers over time the three piers were selected and added to the plot functions. Then the “Define Functions” button was selected and the shear 3-3 was selected for each of the piers. The “display” button at the bottom of the window creates a graph of the response of the piers. In order to analyze this bridge nine models were created each one increasing the period by one second, from non-isolated to a period of eight seconds.

## **6.5. Spectra**

In order to view spectrographs of the earthquakes used Spectra was used. It is a free program, which can be downloaded from [http://moment.mit.edu/r\\_modules.asp](http://moment.mit.edu/r_modules.asp). Spectra can generate graphs of the time history, spectral displacement, velocity, and acceleration for twenty-one earthquake records.

## **6.6. Results**

The bulk of the SAP analysis was performed on the El Centro Earthquake, which hit California on May 18, 1940. It is considered an impulse earthquake because it releases most of its energy in the first few seconds (Figure 19). Because earthquakes are a combination of many random frequencies without a focus on one frequency it can be expected that in general the displacement of the bridge deck should increase as the period of the bridge increases and therefore the stiffness decreases. On the other hand the shear force felt by the columns should decrease. In practice the response of the bridge to El Centro was slightly different than expected.

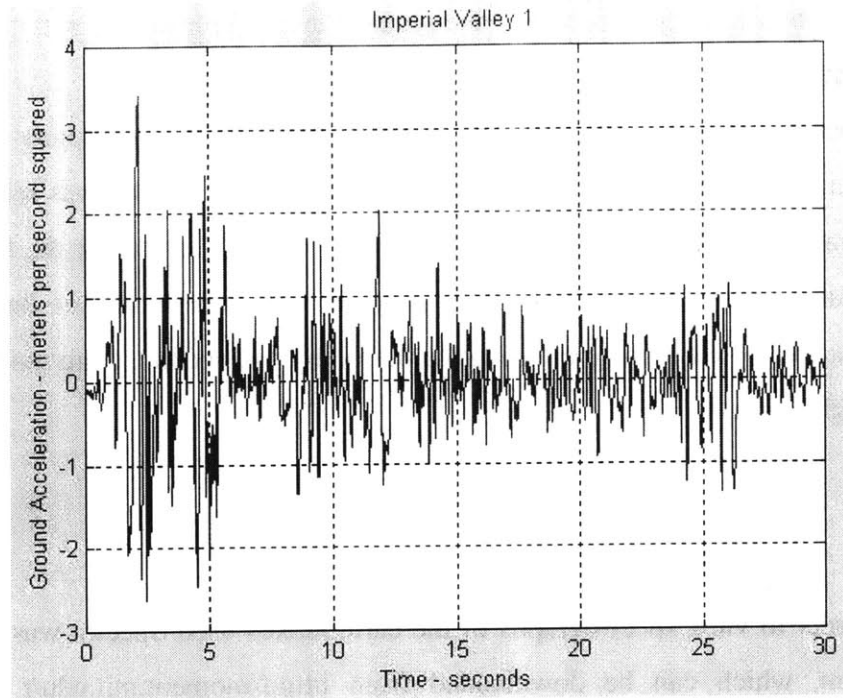


**Figure 19: The ground acceleration in terms of time of El Centro**

The estimated stiffness of the isolator and the stiffness found by SAP corresponded almost perfectly. In the first iteration the SAP stiffness was three times greater than the estimated stiffness. There were two reasons for this. The first is that the columns had an area that was too large in comparison to the length. They were four square meters in area and five meters in length. This caused the columns act more like shear beams than bending beams. The formulation for stiffness used is only true for bending beams. Secondly, the fundamental mode of the bridge was laterally, not longitudinally. This means that the stiffness of the column is reduced from 12 times  $EI$  of  $L$  cubed to 3  $EI$  over  $L$  cubed.

The displacement showed a general upward trend as the period was lengthened as shown in Figure 20 shown below.



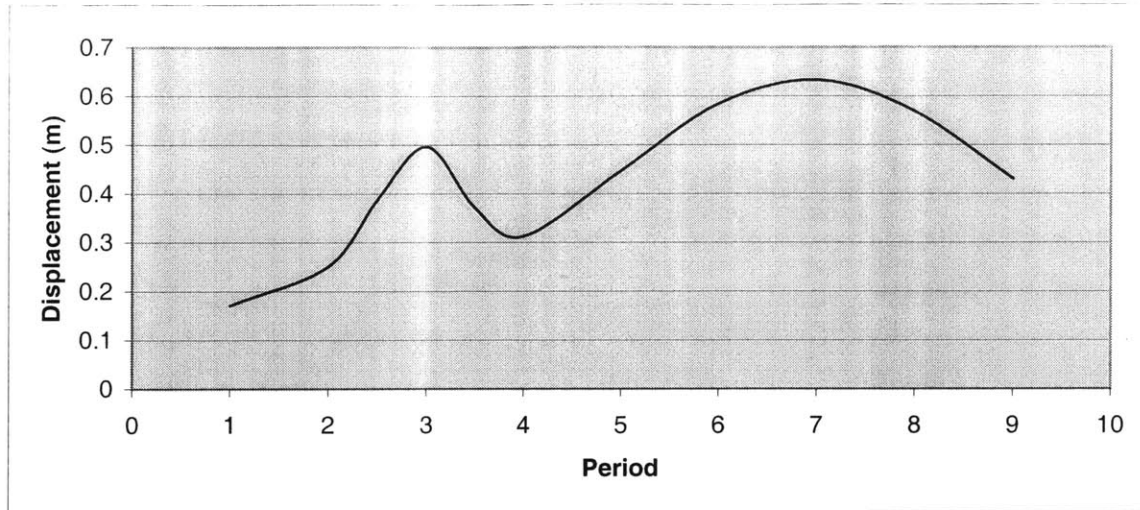


**Figure 20: The response of the bridge to El Centro for different periods**

It is evident that the displacement seems to steadily increase except for the jump at a period of around three seconds. The reason for this jump is not immediately evident. However, the spectrograph of El Centro gives some insight into the reason for this sudden increase in displacement. As Figure 21 shows, the spectral acceleration drops significantly from a period of 1 second to a period of 1.5 seconds then remains mostly constant until dropping again after 3 seconds. Figure 22 gives a better explanation for this displacement increase. For periods in the vicinity of three seconds the displacement increases from about 0.1 meters to 0.4 meters and then settles back down to 0.1 meters when the period reaches 4 seconds. It is possible that this spectral displacement may be the cause of the displacement jump of the bridge. This hypothesis will be tested by examining the spectrograph of the Northridge Earthquake for displacement and acceleration jumps and isolating the bridge accordingly.

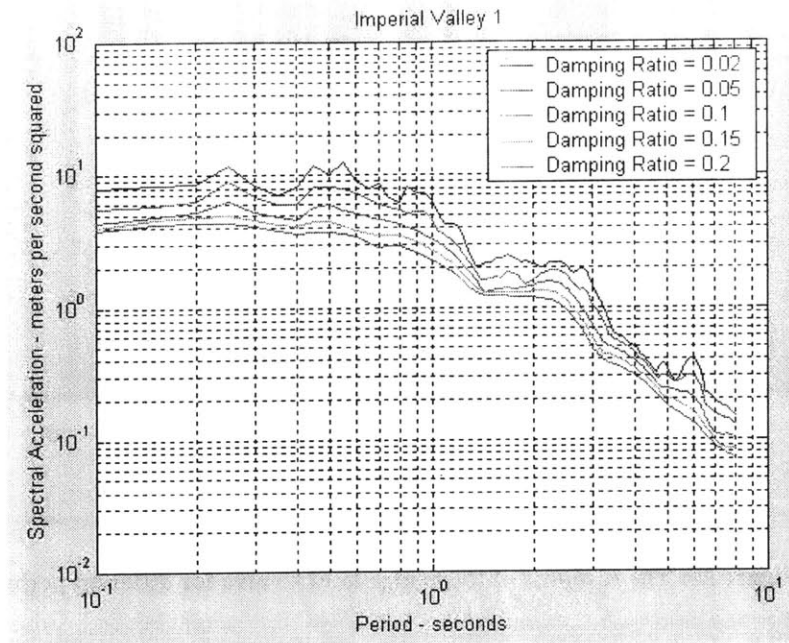


**Figure 21: The spectral acceleration of El Centro**

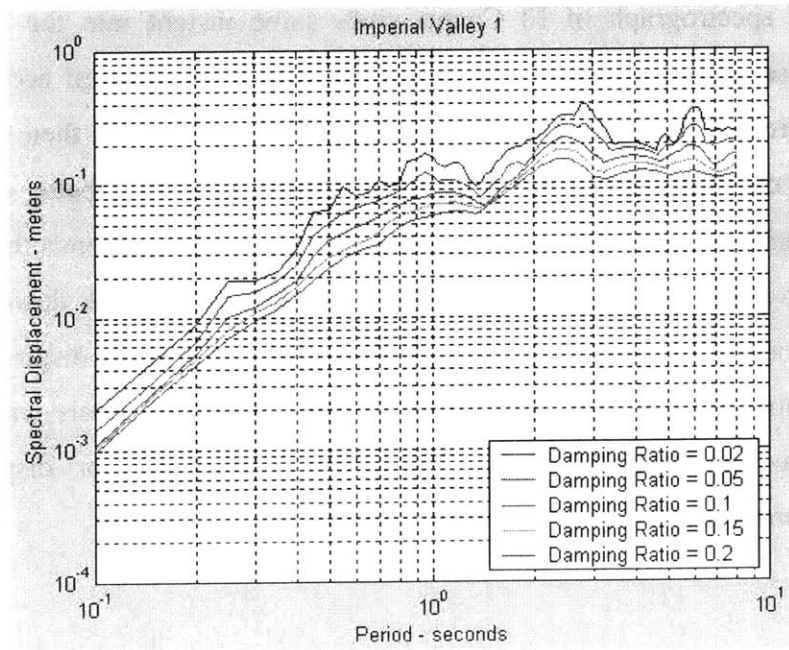


**Figure 22: The spectral displacement of El Centro**

The second question the displacement graph raises is the decrease in displacement for periods greater than seven seconds. There are two possible explanations for this

behavior. The first is that it is some error in SAP due to integration of accelerations in the time history record. Program error is a possibility, but system behavior seems to be more likely. Theoretically if the stiffness of the system were zero the deck would have zero displacement and therefore relative to the ground motion would be exactly opposite. This is the opposite of the SdoF system discussed earlier, which had zero displacement in relation to the ground because it moved with the ground, but had a global displacement exactly the same as the displacement of the ground. There seems to be some critical period length at which point the displacement decreases until it reaches a global zero or a maximum value relative to the ground equal to that of maximum ground displacement. It might seem that this would be the best solution. In theory the deck would feel no force because there would be no acceleration and the columns would feel no shear because the isolators would be so flexible. However, wind loading would cause great displacements and isolator would not have enough restoring force to return the bridge to its original position.

As expected the shear forces in the columns decreases as the period is lengthened. Figure 23 shows the graph of column shear.

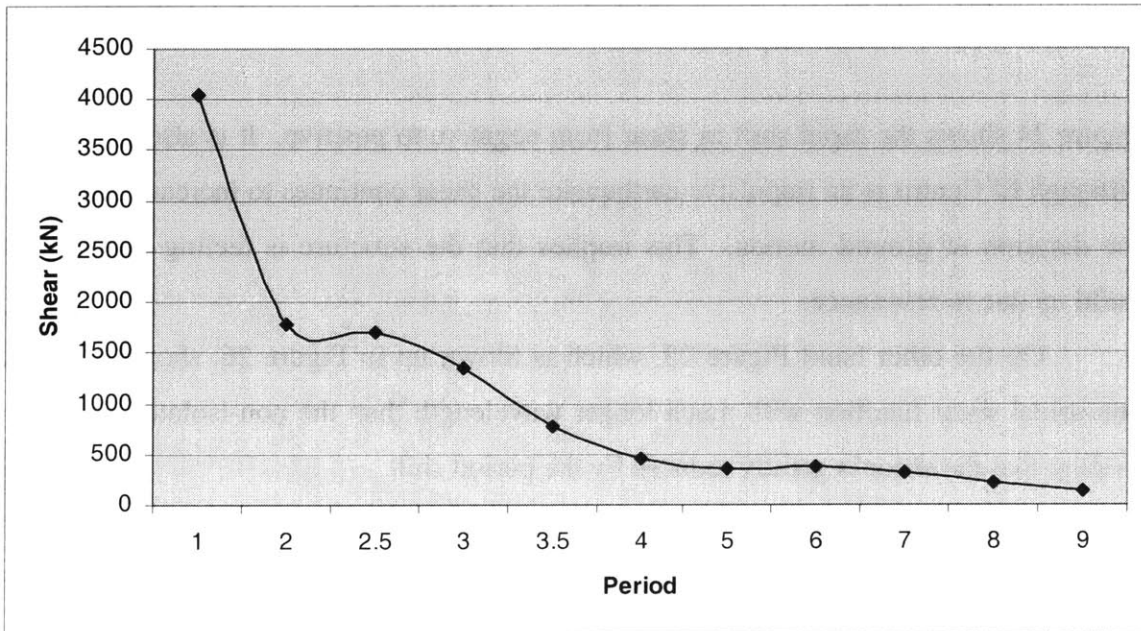
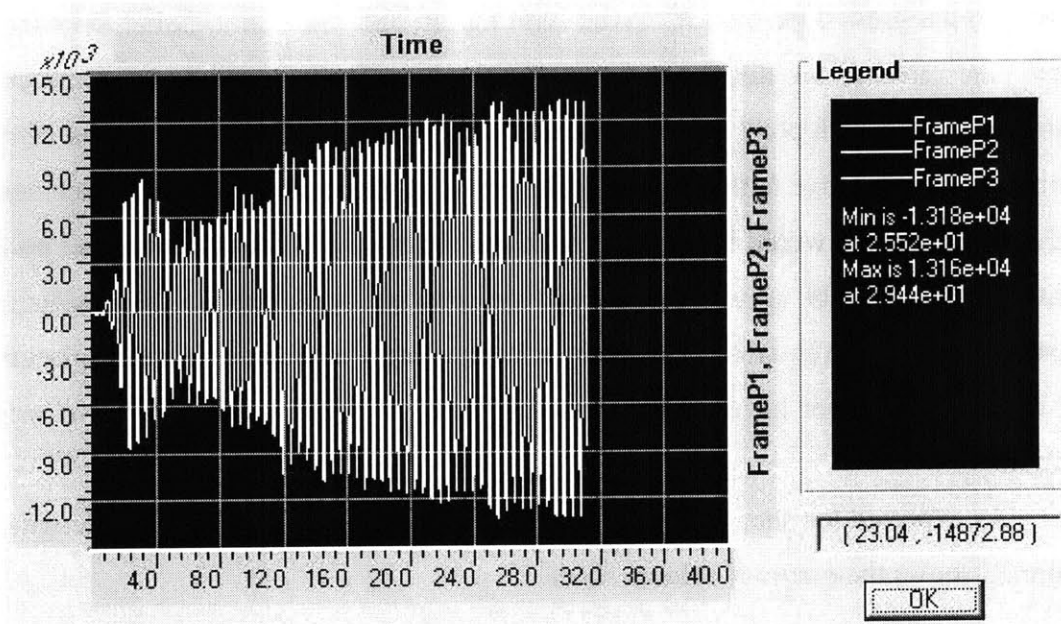


Figure 23: Shear in the columns as a function of the period of the bridge

It seems that the jump in displacement also affects the shear. However, the magnitude of the shear increase does not seem to be as significant as the displacement increase. Figure 23 demonstrates that isolation has a dramatic effect on the magnitude of the shear in piers. The further out the period is shifted the lower the shear in the columns becomes.



**Figure 24: The time history of the shear in the piers in the non-isolated case**

Figure 24 shows the rapid shift in shear from negative to positive. It is also evident that although El Centro is an impulsive earthquake the shear continues to increase throughout the duration of ground motion. This implies that the structure is feeling some energy build up due to resonance.

On the other hand Figure 25, which is blown up in Figure 26, shows a roughly sinusoidal shear function with much longer wavelength than the non-isolated case. It is evident that the shear is greatly reduced by the period shift.

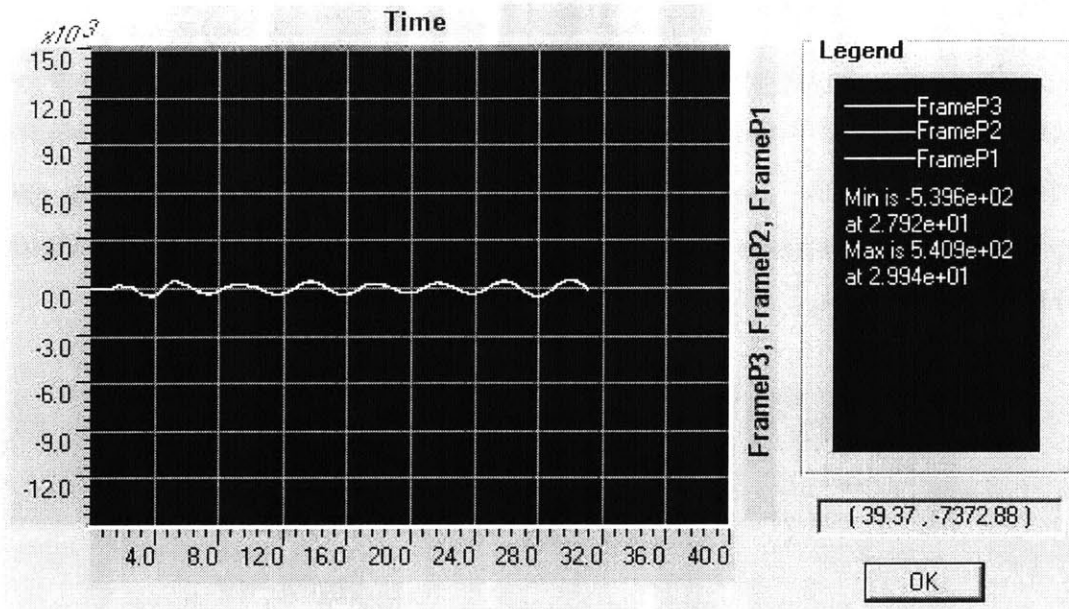


Figure 25: The shear in the piers in the case of a period of 4 seconds. The magnitude of the vertical scale is the same as the non-isolated bridge shown in Figure 24

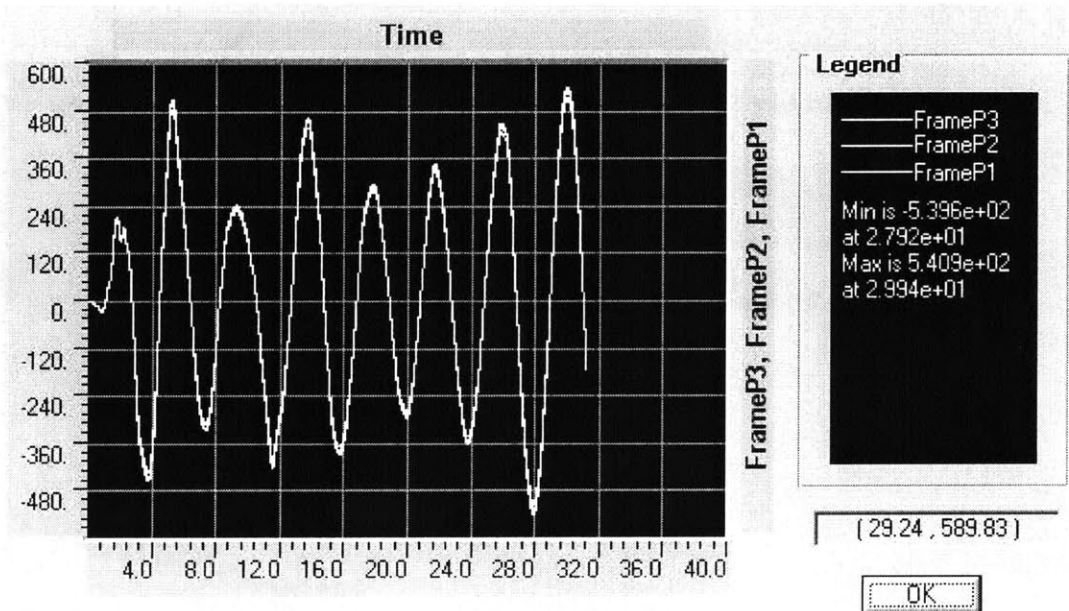


Figure 26: The shear in the piers in the case of a period of 4 seconds zoomed in

## 6.7. Northridge Earthquake

In order to verify the relationship between the spectral acceleration and displacement and the actual displacement the bridge was subjected to the Northridge Earthquake, which hit southern California on January 17, 1994. The spectral displacement and acceleration graphs were examined (pictured in Figure 27, Figure 28, and Figure 29).

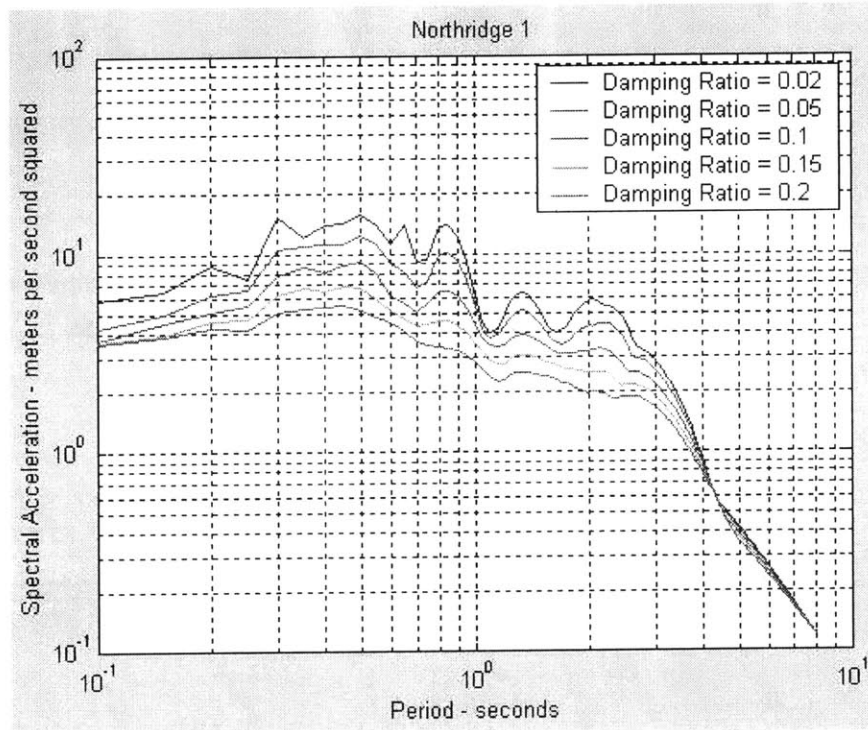


Figure 27: The spectral acceleration of the Northridge Earthquake

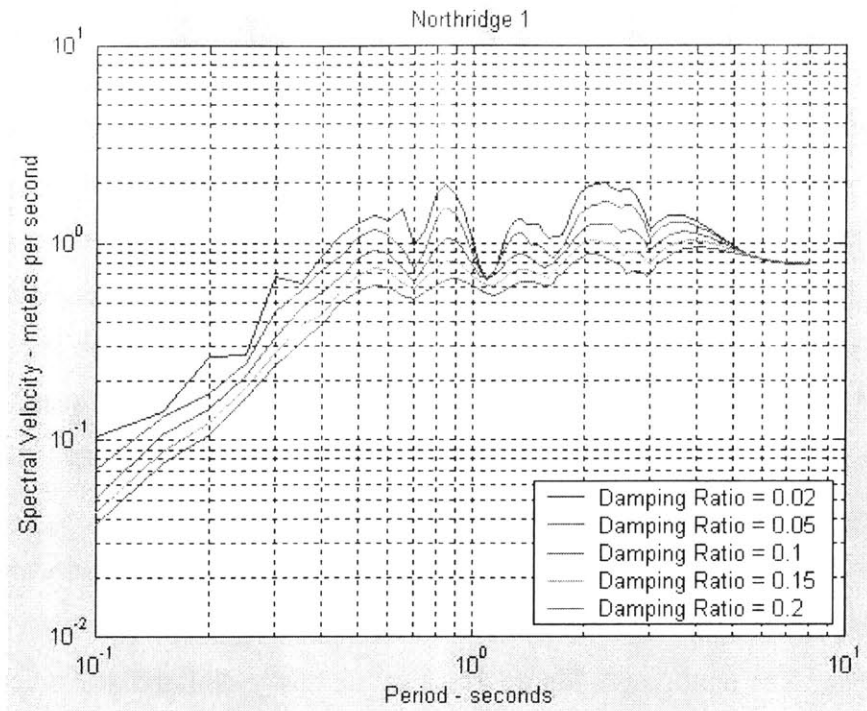


Figure 28: The spectral velocity of the Northridge Earthquake

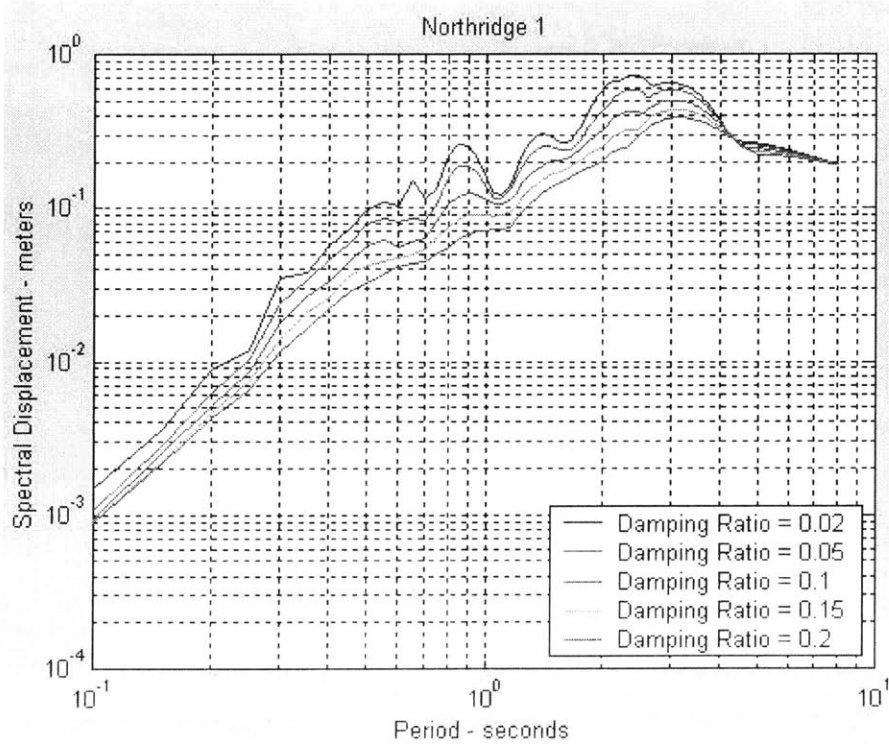


Figure 29: The spectral displacement of the Northridge Earthquake

There seems to be an increase in spectral acceleration, and velocity starting at a period of 1.75 seconds, reaching a maximum at 1.25 seconds, and the decreasing until the period reaches 2 seconds. The displacement begins increasing at 1.75 seconds, reaches a maximum from 2 to 3 seconds and decreases until reaching the same value it as the 1.75 seconds at 3 seconds. Therefore, following the same logic applied to explain the jump in displacement of the bridge isolated to three seconds, it can be assumed that isolating the bridge to 2.25 seconds will give a much greater displacement and a slightly higher shear in the piers than the bridge isolated to either 1.75 seconds or 3 seconds. The following graphs show the results of these periods of isolation.

The first graph, Figure 30, shows the displacement over time for the bridge isolated to a period of 1.75 seconds, a place identified as a low area of all three spectrographs. The next graph, Figure 31, is of the bridge isolated to 2 seconds. At two seconds all three graphs reach maximum values. As expected the displacement is greater than in the first case, almost twice as large in fact.

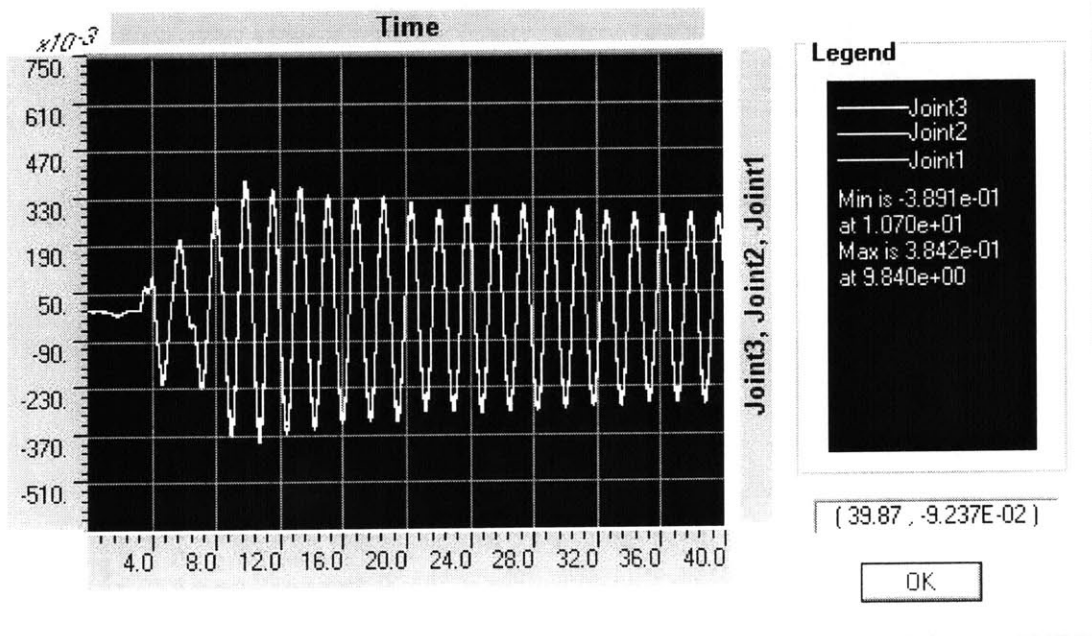
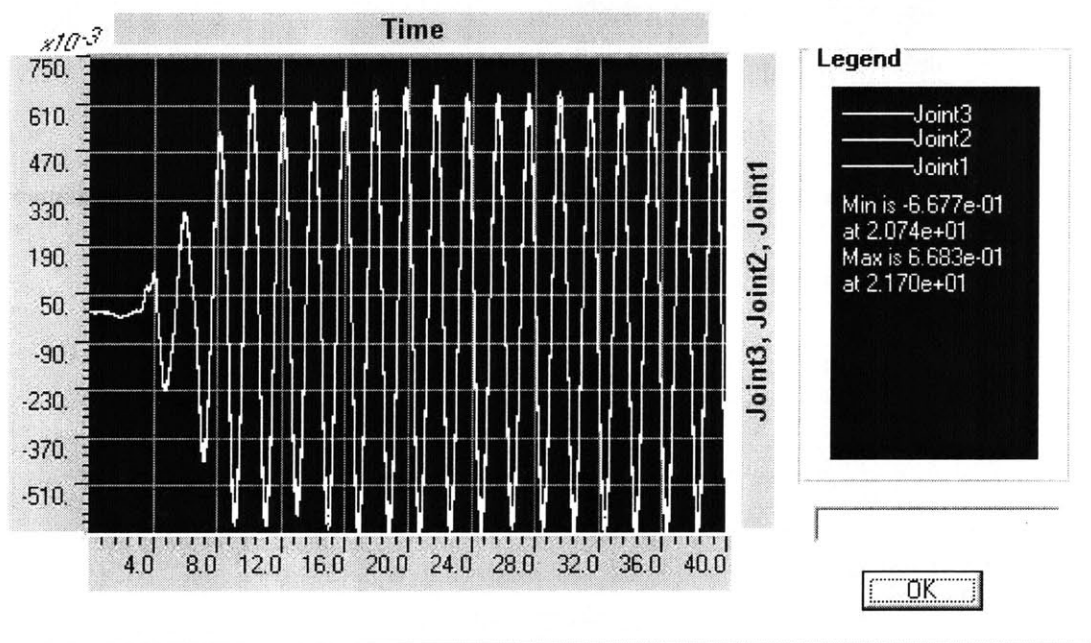


Figure 30: The displacement of the bridge subjected to the Northridge Earthquake and isolated to a period of 1.75 seconds



At three seconds the spectral acceleration and velocity drop off but the spectral displacement remains high. A look at Figure 32 shows that the maximum value of displacement at a three second period is even greater than for two seconds. However, this maximum is only reached during a spike in displacement from 6 to 8 seconds the rest of the graph is consistently lower than the values in the bridge with a period of 2 seconds. Finally, the four-second structure has a displacement graph that looks very similar to the three-second structure, except for the large spike in the three-second case (Figure 33). The rest of the displacement values are of about the same magnitude.



**Figure 31: The displacement of the bridge subjected to the Northridge Earthquake and isolated to a period of 2 seconds**

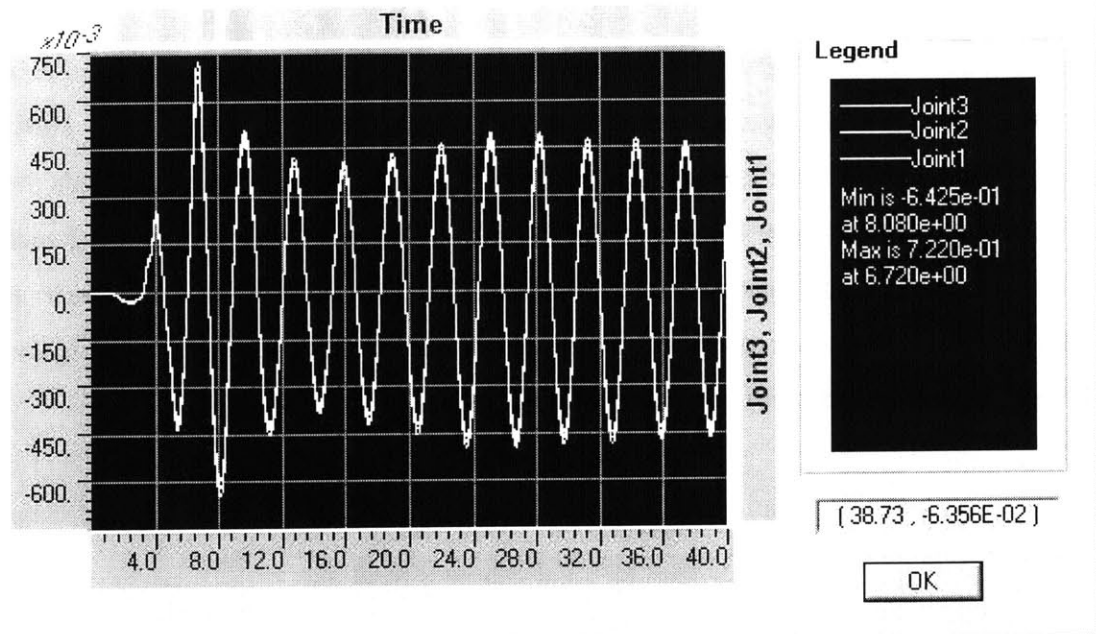


Figure 32: The displacement of the bridge subjected to the Northridge Earthquake and isolated to a period of 3 seconds

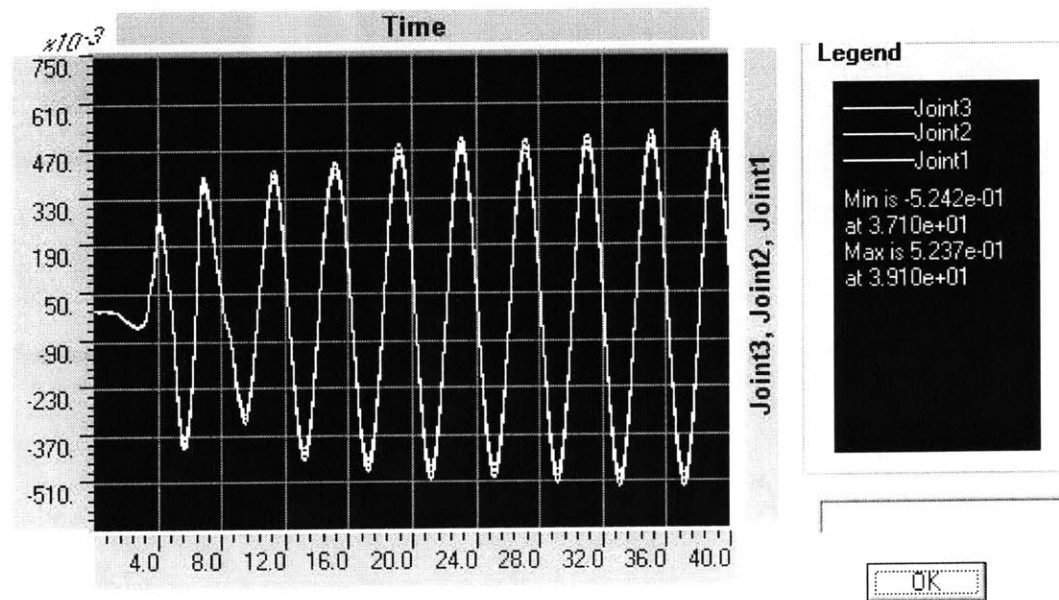


Figure 33: The displacement of the bridge subjected to the Northridge Earthquake and isolated to a period of 4 seconds

## 7. Discussion and Conclusions

This research demonstrates the importance of spectral analysis for seismic design. It is generally agreed that the critical power of seismic events ranges from 0.6 seconds to 1.5 seconds in period [5, 10]. This assessment seems to be true for the base shear in the case of El Centro. The shear in columns drops significantly from the un-isolated case to the two-second isolated structure (Figure 23). If this general rule was followed for El Centro and the structure was isolated say to slightly past 2 seconds the displacement would be significantly increased due to El Centro's spectral displacement increase from 2 to 4 seconds. There is a similar increase in displacement caused by the Northridge Earthquake.

All earthquakes occurring in a certain region will not be exactly the same. For instance all quakes in southern California have not been and will not be exactly like Northridge. However, as discussed in the first chapter the major tectonic plates interact in one of three ways, divergent, convergent and transform zones [1]. Earthquakes in each zone tend to behavior similarly. For example transform zones have a higher probability of seeing lateral strike-slips. Although Maine is not situated on a major fault it still may experience a major earthquake as the New Madrid quake demonstrated. To do a full seismic design for a bridge in Maine it would be useful to gather records of intra-plate quakes like New Madrid and use them for the spectral analysis.

In the case of a quake designed for El Centro and Northridge it is recommended the structure be isolated to 1.75 seconds if displacement is a major concern. If column shear is more important, isolating the bridge to 4 seconds would greatly reduce shear while only increasing the displacement by about 20 centimeters. The design codes limit the maximum isolation to 7 seconds, so 4 seconds is not too extreme [11].

## References:

1. Keller, Edward and Nicolas Pinter. Active Tectonics: Earthquakes, Uplift, and Landscape. New Jersey: Prentice Hall, 2002.
2. Key, David. Earthquake design practice for buildings. London: Thomas Telford, 1988.
3. Takewaki, Izuru. "Frequency domain modal analysis of earthquake input energy to highly damped passive control structures." Earthquake Engineering and Structural Dynamics 33 (2004): 575-590.
4. Komodromos, P. Seismic Isolation for Earthquake Resistant Structures. Boston: WIT Press, 2000.
5. Wesolowsky, Micheal, and John Wilson. "Seismic isolation of cable-stayed bridges for near-field ground motions." Earthquake Engineering and Structural Dynamics 32 (2003): 2107-2126.
6. Naeim, Farzad and James Kelly. Design of seismic isolated structures: from theory to practice. New York: John Wiley, 1999.
7. Karim, Kazi and Fumino Yamazaki. "A simplified method of constructing fragility curves for highway bridges." Earthquake Engineering and Structural Dynamics 32 (2003): 1603-1626.
8. Connor, Jerome. Introduction to Structural Motion Control. New Jersey: Prentice Hall, 2003.
9. ENR – Northridge Aftermath: Aftershocks Continue. Engineering News-Record. 30 April 2004. <http://enr.construction.com/news/transportation/archives/040126.asp>
10. Dicleli, Murat. "Seismic Design of Lifeline Bridge using Hybrid Seismic Isolation." Journal of Bridge Engineering 7 (2002): 94-103.
11. Roussis, Panayiotis, Micheal Constantinou, Mustafa Erdik, Eser Durukal, and Murat Dicleli. "Assessment of Performance of Seismic Isolation System of Bolu Viaduct." Journal of Bridge Engineering 8 (2003): 182-190.
12. Lee, Zheng-Kuan, Tzu-Hsiu Wu, and Chin-Hsiung Loh. "System identification on the seismic behavior of an isolated bridge." Earthquake Engineering and Structural Dynamics 32 (2003): 1797-1812.
13. The library are the University of Texas website. 29 April 2004. <[http://www.lib.utexas.edu/maps/middle\\_east\\_and\\_asia/turkey\\_nw\\_2002.jpg](http://www.lib.utexas.edu/maps/middle_east_and_asia/turkey_nw_2002.jpg)>

14. Literature Review of the Observed Performance of Seismically Isolated Bridges. The University of Buffalo. 20 April 2004.

[http://64.233.161.104/search?q=cache:moJJbE40Q8cJ:mceer.buffalo.edu/publications/res+acc0m/0001/rpa\\_pdfs/06lee-bridges.pdf+Bai-Ho+Bridge&hl=en](http://64.233.161.104/search?q=cache:moJJbE40Q8cJ:mceer.buffalo.edu/publications/res+acc0m/0001/rpa_pdfs/06lee-bridges.pdf+Bai-Ho+Bridge&hl=en)

15. The library are the University of Texas website. 29 April 2004.

<[http://www.lib.utexas.edu/maps/middle\\_east\\_and\\_asia/taiwan\\_pol92.jpg](http://www.lib.utexas.edu/maps/middle_east_and_asia/taiwan_pol92.jpg)>

16. NCEDC: EVT\_FAST Request Form website. Berkeley University. 15 April 2004.

<[http://quake.geo.berkeley.edu/ncedc/evt\\_fast\\_form.html](http://quake.geo.berkeley.edu/ncedc/evt_fast_form.html)>